DRAFT.

Riprap Stability Versus Monochromatic and Irregular Waves

By

Laurie Lynn Broderick

B.S. June 1979, Oregon State University

A Thesis submitted to

The Faculty of

The Graduate School of Engineering and Applied Science
of The George Washington University in partial satisfaction
of the requirements for the degree of Master of Science

April 1984

RIPRAP STABILITY

ABSTRACT:

A three-phase study of riprap stability was conducted at the U.S. Army Coastal Engineering Research Center. Phase One was large-scale tests of riprap stability using monochromatic waves (Ahrens, 1975). Phase Two was small-scale tests of riprap stability that replicated the Phase One, large-scale tests at a 1:10 Froude scale (Broderick and Ahrens, 1982). Phase Three was small-scale tests of riprap stability using irregular waves. The test setup and procedures, data analysis, and results are discussed. The small-scale tests, Phase Two, gave more conservative estimates of zero-damage wave heights and wave runup than those predicted by the large-scale test results, Phase One. The results from the Phases Two and Three tests showed that if the significant wave height is used in the standard stability equation, the structure would be underdesigned if the design guidance was based on monochromatic wave tests. If the two conclusions are considered and design guidance is based on laboratory tests done at small scale with monochromatic waves, the significant wave height is recommended to be used in design computation when designing a riprap revetment.

Acknowledgment

Research for this thesis was done at the U. S. Army Engineer Waterways Experiment Station's Coastal Engineering Research Center (CERC) now located in Vicksburg, Mississippi, although data were collected while CERC was located at Fort Belvoir, Virginia. The conclusions and findings reported in this thesis are those of the author and are not to be construed as an official Department of the Army position unless so designated by other authorized documents.

There are many people who deserve thanks and credit for the quality of this thesis--the technicians, Lou Meyerle, Fred Lago, Bob Stafford and George Simmons, who spent hours and days collecting the data; Ken Hassenflug who ensured that the computer was working so that data could be collected and analyzed and irregular waves could be generated. Special thanks go to John Ahrens who was an advisor through the initial days of this study and later a sounding board for my ideas. John also collected data and performed the original analysis of the Phase I test (large-scale tests) and initiated the Phase II test (small-scale test).

TABLE OF CONTENTS

List of Illustrations

List of Tables

List of Symbols

a, b	dimensionless coefficients
Cg	wave celerity
d	water depth at toe of structure
D	damage to the revetment
D'	dimensionless damage
D_{50}	median riprap diameter
D_{15}(riprap)	diameter of the 15 percent finer of the riprap
D_{85}(filter)	diameter of the 85 percent finer of the filter
g	acceleration due to gravity
H	wave height
L	wave length
(ℓc)r	characteristic linear dimension of the riprap
N_s	stability number
r_t	roughness term
R	runup
R_E, R_N	Reynolds number
S	distance from the toe of structure to the wave generator blade
T	wave period
Vw	velocity of the water
W	riprap weight
W_{50}	median riprap weight
W_d	wave burst duration
β	angle of incidence of wave attack
γ_r	unit weight of the riprap
γ_w	unit weight of the water
Δ	shape of the riprap
θ	revetment slope from the horizontal
μ	dynamic viscosity of the water
ν	kinematic viscosity of the water

List of Symbols (Continued)

ξ	surf parameter
$(\xi_c)_r$	characteristic linear dimension of the surface roughness of the riprap
ρ_r	mass density of the riprap
ρ_w	mass density of the water

Introduction

Riprap is a graded quarry stone commonly used as a revetment to protect soil embankments from wave and current attack. Quarry stone can provide a stable and usually durable material for revetment armor and is relatively low in cost when compared to other alternatives. In general, design guidance for riprap is based on small-scale model studies conducted using monochromatic waves (waves of constant height and period). Questions have been raised as to the reliability of such guidance because of scale effects and the use of monochromatic waves in testing.

Scale effects are the differences that occur between small-scale test results and prototype-scale test results if the small-scale tests replicate the prototype tests. If the magnitude of the scale effects is known, small-scale test results can be extrapolated to prototype scale with confidence. Monochromatic waves seldom represent naturally occurring wave trains, but it has been only in the last few years that irregular waves can be satisfactorily generated in the laboratory. The ideal solution would be to conduct all the tests at prototype scale with irregular waves; but facilities for such purposes are not readily available and are very expensive to build and operate.

To deal with the problem of scale effects and the application of monochromatic waves instead of irregular waves, the Coastal Engineering Research Center (CERC) of the U. S. Army Engineer Waterways Experiment Station (WES) conducted a three-phase study on riprap stability. In Phase One large-scale tests of riprap stability (Ahrens, 1975) were conducted in CERC's large wave tank (LWT). Wave heights in the LWT tests exceeded 1-1/2 meters in some instances and can be regarded as representing prototype scale for some field conditions. In Phase Two small-scale tests were conducted which at a 1:10-Froude scale replicated the large-scale tests (Broderick and Ahrens, 1982). The first two phases were conducted using monochromatic waves. Phase Three involved irregular waves and thus provided a more realistic representation of natural wave conditions. Phase Three tests were conducted at the same scale and in the same facility as the Phase Two tests.

The laboratory setup, test procedures, and data analysis are presented for each of the three phases of testing. Results of Phases One and Two are compared to evaluate the magnitude of the scale effects. Phases Two and Three are compared to evaluate the effects of monochromatic waves as opposed to those of irregular waves. The results of this three-phase study are compared to other laboratory studies that address the question of scale effects and monochromatic waves versus irregular waves. Phase Three results are extrapolated to prototype scale using the scale effects information from Phases One and Two (see Figure 1).

The Phase I data and initial analysis are not part of this thesis; it was a CERC study conducted by John Ahrens (1975). The Phase I data have been included as though a part of the thesis in order to make the thesis complete.

Background Information

Scale Effects Controversy

The motivation behind this study (at least Phases One and Two) was the controversy over whether scale effects exist in laboratory work on riprap stability at the scales normally tested. An early study conducted by WES (Dai and Kamel, 1969) on the scale effects associated with rubble-mound breakwaters concluded that little, if any, scale effects existed. Then a CERC study (Thomsen, Wholt, and Harrison, 1972) concluded that for a rubble-mound revetment scale effects exist, and the small-scale test results could be 50 percent more conservative than the prototype tests.

What's the answer? Do scale effects exist or at what scale do scale effects become significant? Within the Corps of Engineers this question could not be answered; WES said no scale effects exist and CERC said scale effects do exist. The difference between the results of the WES and CERC study could simply be that the WES study dealt with breakwaters and the CERC study dealt with revetments. This explanation is not accepted by other laboratories, i.e., the Hydraulic Research Station personnel, Wallingford, England, definitely think that scale effects do not exist (Pitt and Ackers, 1982). Thus, this study was conducted to answer the question, do scale effects exist?

RIPRAP STABILITY TEST AN OVERVIEW

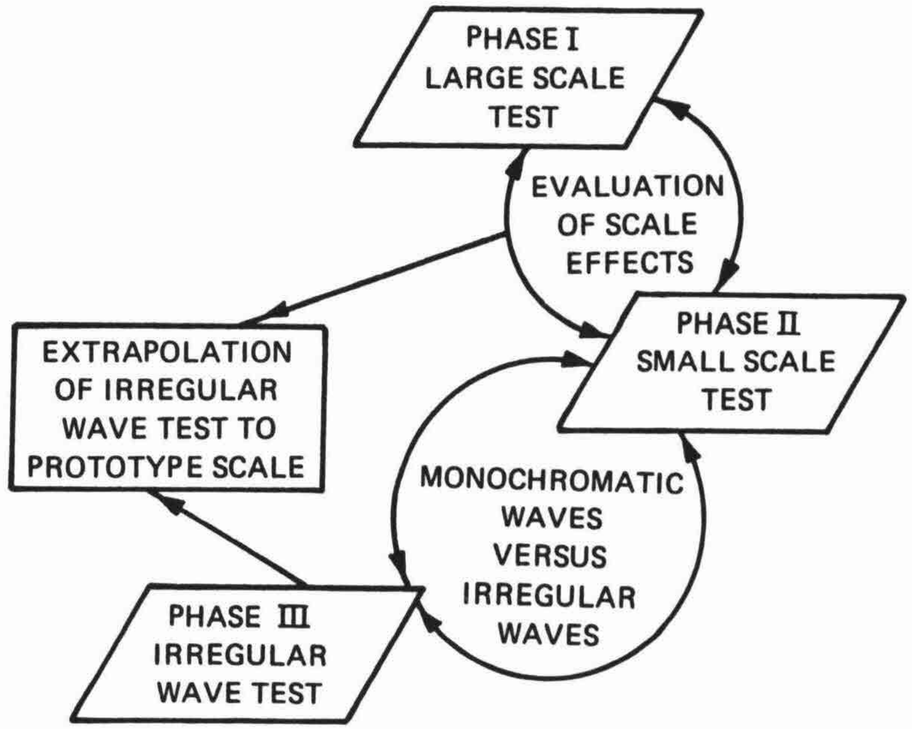

Figure 1. Riprap Stability Test, An Overview

Modeling

When a rubble-mound revetment is subject to the attack of gravity waves, the stability of the riprap is a function of the following variables (Hudson, et al., 1979 and Vernard and Street, 1976):

d = depth of water
D = damage to the revetment
g = acceleration due to gravity
H = wave height
$(\ell c)_r$ = characteristic linear dimension of the riprap
L = wave length
Vw = velocity of water that impinges on and flows around the riprap
β = angle of incidence of wave attack
Δ = shape of the riprap
θ = revetment slope from the horizontal
μ = dynamic viscosity of the water
$(\xi_c)_r$ = characteristic linear dimension of the surface roughness of the riprap
ρ_r = mass density of the riprap
ρ_w = mass density of the water

Thus, by the π theorem

$$f' \left[Vw,\ g,\ \rho_r,\ \rho_w,\ \mu,\ H,\ L,\ d,\ (\ell c)_r,\ (\xi_c)_r,\ \beta,\ \Delta,\ \theta,\ D\right] = 0 \quad \text{(Eq. 1)}$$

and

$$f'' \left[\frac{Vw}{g^{1/2}(\ell c)_r^{1/2}},\ \frac{Vw(\ell c)_r}{\mu/\rho_w},\ \frac{\rho_w}{\rho_r},\ \frac{(\ell c)_r}{d},\ \frac{H}{L},\ \frac{d}{L},\ \frac{(\xi_c)_r}{(\ell_c)_r},\ \beta,\ \Delta,\ \theta,\ D\right] = 0 \quad \text{(Eq. 2)}$$

The forces that act on the riprap surface during wave attack are gravity, inertia, form drag, and surface drag (viscous). Gravity and form drag forces are the predominant forces for this type of phenomenon and stability models of rubble mound revetments are thus designed based on Froude modeling laws. Inertial forces are a result of the pressure gradient in the water. When

Froude modeling laws are used the inertia forces relative to gravity forces are scaled nearly correctly; the form drag forces relative to gravity forces are scaled nearly correctly (depending upon the shape, weight, and the specific gravity of the riprap and the size of the wave) and viscous forces relative to gravity forces are scaled incorrectly.

To have true similitude between the model and prototype the following relationships must hold. The subscript m is for model conditions and the subscript p is for prototype conditions:

$$\left(\frac{Vw}{(\ell c)_r^{1/2} g^{1/2}}\right)_m = \left(\frac{Vw}{(\ell c)_r^{1/2} g^{1/2}}\right)_p \qquad \text{(Eq. 3a)}$$

$$\left(\frac{\rho_w}{\rho_r - \rho_w}\right)_m = \left(\frac{\rho_w}{\rho_r - \rho_w}\right)_p \qquad \text{(Eq. 3b)}$$

$$\left(\frac{Vw(\ell_c)_r}{\mu/\rho_w}\right)_m = \left(\frac{Vw(\ell c)_r}{\mu/\rho_w}\right)_p \qquad \text{(Eq. 3c)}$$

$$\left(\frac{(\ell c)_r}{d}\right)_m = \left(\frac{(\ell c)_r}{d}\right)_p \qquad \text{(Eq. 3d)}$$

$$\left(\frac{H}{L}\right)_m = \left(\frac{H}{L}\right)_p \qquad \text{(Eq. 3e)}$$

$$\left(\frac{d}{L}\right)_m = \left(\frac{d}{L}\right)_p \qquad \text{(Eq. 3f)}$$

$$\left(\frac{(\xi_c)_r}{(\ell c)_r}\right)_m = \left(\frac{(\xi_c)_r}{(\ell c)_r}\right)_p \qquad \text{(Eq. 3g)}$$

$$\beta_m = \beta_p \qquad \text{(Eq. 3h)}$$

$$\Delta_m = \Delta_p \qquad \text{(Eq. 3i)}$$

and

$$\theta_m = \theta_p \qquad \text{(Eq. 3j)}$$

Since stability models are designed based on Froude's law and are constructed with geometric similitude (without distorted linear scales), all the above relationships can be satisfied except those indicated by Equation 3c (Reynolds number) and Equation 3g (surface roughness of the riprap). Viscous forces can be made neglibible if the linear scale is selected so that the Reynolds number is not too small. If a rough, turbulent flow regime can be maintained in both the model and the prototype, Reynolds numbers should be large enough so that viscous effects will be negligible. The effects of surface roughness on ordinary quarrystone are negligible at prototype scale and can be made negligible in the model by using relatively smooth riprap.

In Equation 2, the Froude number (Equation 3a) and the density ratio (Equation 3b) can be combined. This is done since the stability of the rubble-mound revetment is determined to a considerable extent by the relative magnitudes of the form drag and submerged weight of the riprap.

$$\left(\frac{Vw}{g^{1/2}(\ell c)_r^{1/2}}\right)\left(\frac{\rho_w^{1/2}}{(\rho_r - \rho_w)^{1/2}}\right) = f'''\left[\frac{Vw(\ell c)_r}{\mu/\rho_w}\ ,\ \frac{(\ell c)_r}{d}\ ,\ \frac{H}{L}\ ,\ \frac{d}{L}\ ,\ \frac{(\xi_c)_r}{(\ell_c)_r}\ ,\ \beta\ ,\ \Delta\ ,\ \theta\ ,\ D\right] \qquad \text{(Eq. 4)}$$

The velocity, Vw, of the waves or of the water particles that impinge on the riprap during wave attack is not easily measured during the tests, so Vw is replaced by the relation $Vw = f(gH)^{1/2}$. The reason Vw can be replaced by the relationship $(gH)^{1/2}$ is that $(gH)^{1/2}$ is a measure of the celerity of the wave and as the wave approaches breaking, the water particle velocity approaches the wave celerity. Other convenient substitutions are:

ν = kinematic viscosity, μ/ρ_w ;
γ_r = specific weight of riprap, $\rho_r g$;
γ_w = specific weight of water, $\rho_w g$; and
W = weight of riprap $f\left[(\ell c)_r^3 w_r\right]$.

With these substitutions Equation 4 becomes

$$\frac{(\gamma_r)^{1/3} H}{\left(\frac{\gamma_r}{\gamma_w} - 1\right) W^{1/3}} = f''''\left[\frac{g^{1/2} H^{1/2} (\ell c)_r}{\nu}\ ,\ \frac{(\ell c)_r}{d}\ ,\ \frac{H}{L}\ ,\ \frac{d}{L}\ ,\ \frac{(\xi_c)_r}{(\ell_c)_r}\ ,\ \beta\ ,\ \Delta\ ,\ \theta\ ,\ D\right] \qquad \text{(Eq. 5)}$$

Equation 5 can be further simplified if Reynolds numbers are large enough to render viscous forces negligible, the model riprap geometrically models the prototype riprap, surface texture of the model riprap is sufficiently smooth relative to the prototype, and the angle of wave attack in the model and the prototype are the same:

$$\frac{H}{\left(\frac{W}{\gamma_r}\right)^{1/3}\left(\frac{\gamma_r}{\gamma_w} - 1\right)} = f^V\left[\frac{H}{L}, \frac{d}{L}, \theta, D\right] \qquad \text{(Eq. 6)}$$

The term on the left in Equation 6 is the stability number, N_s, as defined by Hudson (1958).

$$N_s = \frac{H}{\left(\frac{W}{\gamma_r}\right)^{1/3}\left(\frac{\gamma_r}{\gamma_w} - 1\right)} \qquad \text{(Eq. 7)}$$

The stability number is a measure of the severity of the wave attack on a structure and takes into account both the wave height and the material when the stability number is used as the independent variable and plotted versus a variable (such as damage) data trends are established. These trends can then be used as predictive tools in design. In this thesis the damage trends are established using the stability number and damage caused to the revetment (see Figure 9).

Laboratory Setup and Test Procedures

Phase One, Large Wave Tank Tests

Phase One tests were conducted in CERC's large wave tank (LWT). The LWT was 193.5 meters long, 4.6 meters wide and 6.1 meters deep. The still-water level was 4.6 meters for all the LWT tests. Side boards were placed at the shoreward end of the tank to increase the height of the revetment test structures so all the wave runup could be contained within the tank. The toe of the individual structures was from 118.9 to 137.2 meters away from the generator blade. The distance depended on the slope of the embankment (see Figure 2). Only monochromatic waves could be generated in the LWT.

Core material of the embankment was bank-run gravel and was considered impermeable to wave attack. A filter material with a thickness of 15 to

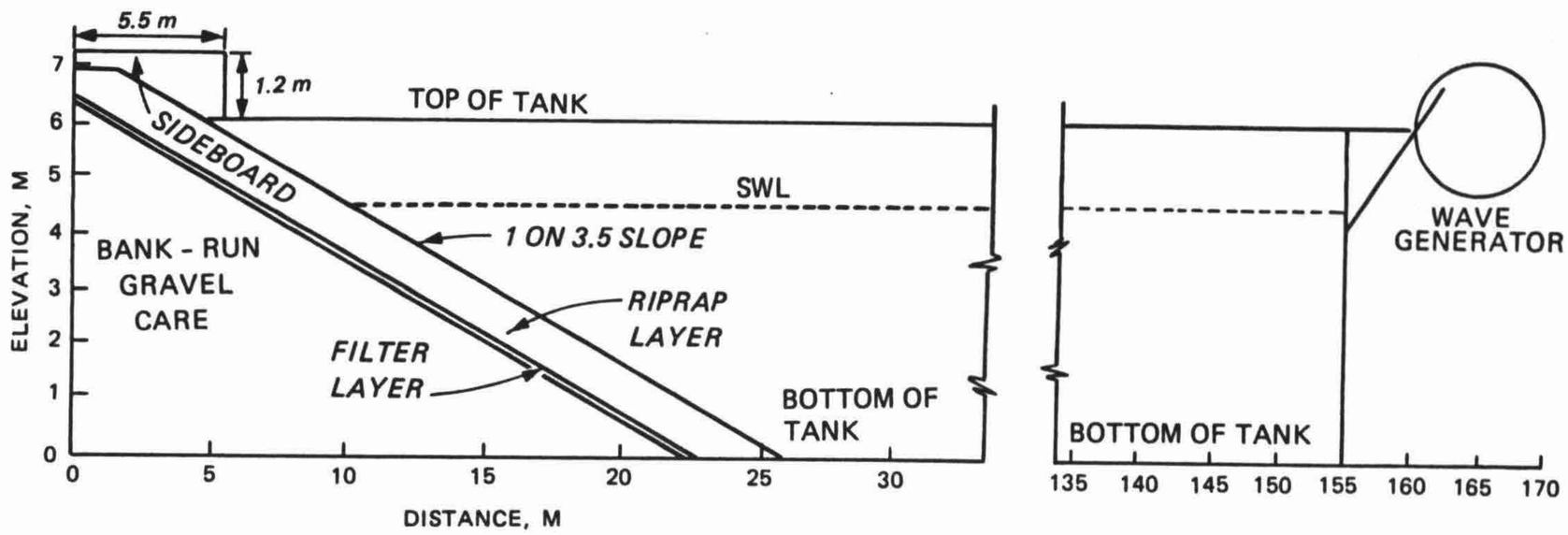

Figure 2. Phase One Test Setup

20 centimeters covered the embankment core. Gradation of the filter material was such that the ratio of the 15 percent finer diameter of the riprap to the 85 percent finer diameter of the filter was usually less than four but always less than five.

$$\frac{D_{15}(\text{Riprap})}{D_{85}(\text{Filter})} \leq 5 \qquad \text{(Eq. 8)}$$

The riprap (a diorite with a specific gravity of 2.71 was placed on top of the filter layer. This diorite generally has a blocky to angular shape. Gradation of the riprap was that recommended in two U. S. Army Corps of Engineer Engineering Manuals (EM 1110-2-2300 and 1110-2-1614). The maximum stone weight was no more than four times the median stone weight, W_{50} , and the minimum stone weight was no less than one-eighth the median stone weight.

$$\frac{1}{8} W_{50} \leq W \leq 4\ W_{50} \qquad \text{(Eq. 9)}$$

where W is the weight of any stone. There were three groups of riprap in the large-scale test each having a different median stone weight but the same gradation (the median stone weights were 12.2 kgs, 34 kgs, or 54.4 kgs). Figure 3 summarizes the gradations of the filter material and the riprap materials used in Phase One. The embankment slope was also varied for the large-scale test, the slope being either 1:2.5, 1:3.5, or 1:5. The largest stone, W_{50} = 54.4 kgs , was tested only on the 1:3.5 slope.

Several wave periods were tested: 2.8, 4.2, 5.7, 8.5, and 11.3 seconds. The 2.8-second wave was not tested if the maximum wave height that could be generated was too small to cause extensive damage to the embankment. The wave heights all were determined prior to building the embankment. Wave heights were measured where the toe of embankment slope would be built during the stability test, with a wave absorber installed to diminish wave reflection. Wave heights were measured before construction of the embankment so the wave height used in the data analysis did not include the re-reflected energy, i.e. wave energy reflected from the embankment and then reflected back to the structure from the wave board. During the stability test the waves were generated in bursts so the wave re-reflection was reduced. The burst length was determined by dividing twice the distance from the blade to the toe of the embankment by the group celerity of the waves.

There was a correction applied to the wave height in the large-scale test because of the "last wave effect" (Madsen 1970 and Ahrens 1975). The "last wave

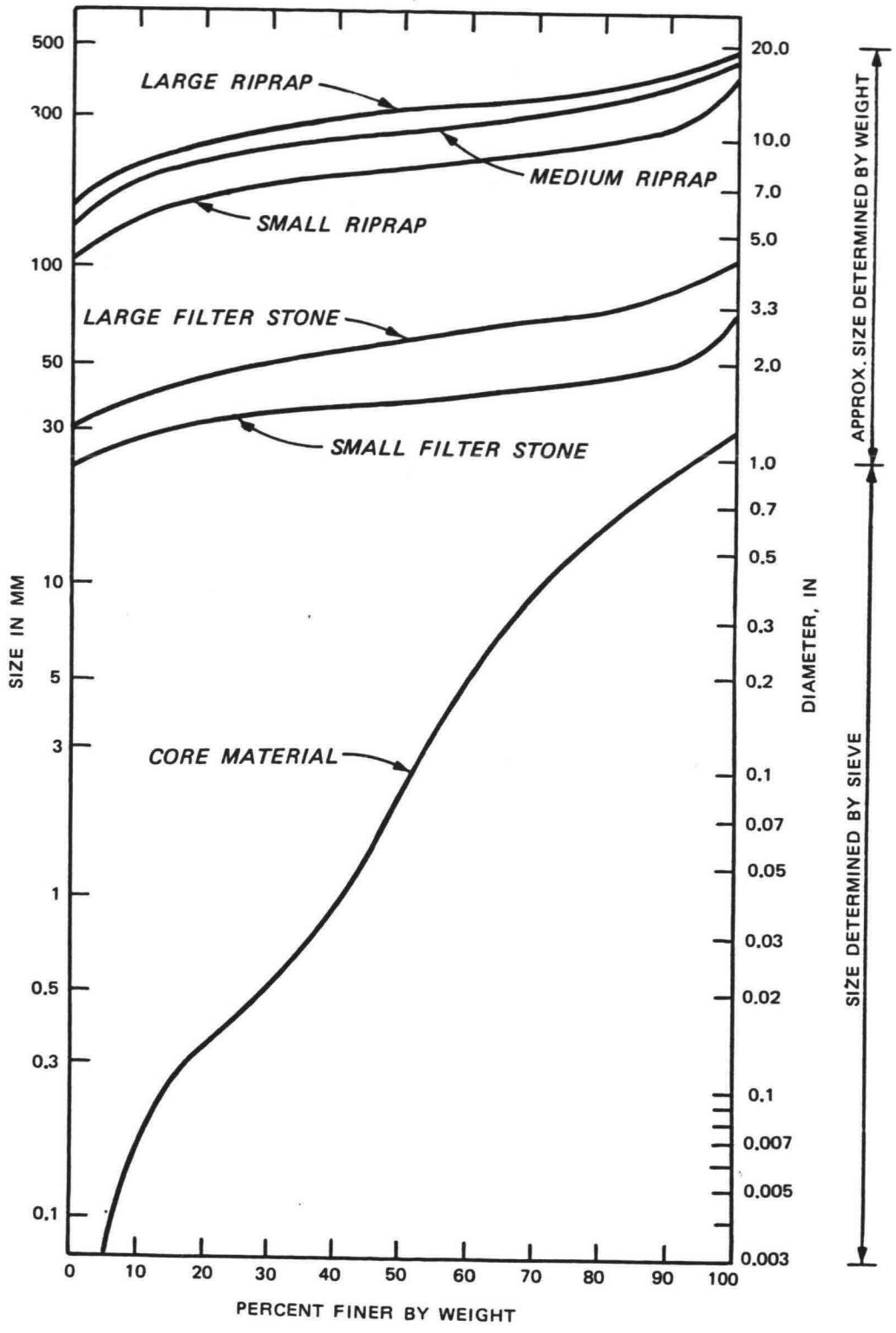

Figure 3. Phase One Gradation of Riprap, Filter and Core Material

effect" refers to the occurrence of one to three waves noticeably higher than the modal wave heights. the number of higher waves that occurred, one to three, is related to the relative water depth d/gT^2 , where T is the wave period. The term "last wave effect" is used because the highest wave usually appears at the end of the burst, although a high wave would usually occur near the beginning of the burst. The highest waves would bracket the smaller waves of almost uniform height, the modal height. The higher waves caused more stone movement to occur so a correction was made to the modal wave height (the corrected wave height was used in the data analysis). The magnitude of the correction was established by laboratory data and was related to the relative water depth (see Ahrens, 1975). The correction decreased from 1.1 for a wave period of 2.8 seconds to 1.04 for a wave period of 11.3 seconds. The "last wave effect" is partially explained by the starting and stopping positions of the generator blade. In the LWT the blade starts and stops in the center of its total stroke which is the point of maximum water particle velocity, thus enhancing transient phenomenon. In the small wave tank used for Phases Two and Three, no correction was made to the wave height for the "last wave effect" because none was needed. In the small wave tank the blade starts and stops in the most rearward position which is where the water particle velocities are zero, thus surpressing transient effects.

During the Phase One study the following test procedures were followed:

1. Place and compact core material;
2. Survey surface profile of the core;
3. Place and smooth filter material;
4. Survey surface profile of the filter;
5. Place riprap by dumping from a skip (which represents field procedures);
6. Survey surface profile of the riprap (reference survey);
7. Run a series of wave bursts (same wave height and period) until no further stone movement was detected;
8. Survey surface profile of the riprap;
9. Increase the wave height approximately 10 percent and repeat Steps 7 and 8;
10. Repeat steps 7, 8, and 9 until failure; failure is defined when enough riprap is shifted to expose the filter material;
11. Survey surface profile of the riprap;
12. Remove the riprap material and survey the damage filter layer;

Table 1. Phase I Test Conditions

Embankment Slope	Median weights of riprap: Small 12.2 kgs	Intermediate 34 kgs	Large 54.4 kgs
1 on 2.5	tested	tested	untested
1 on 3.5	tested	tested	tested
1 on 5	tested	tested	untested

The SWL (d) was 4.6 meters for all Phase I tests.
The wave periods (T) tested were: 2.8, 4.2, 5.7, 8.5, and 11.3 seconds.

Table 2. Phase II Test Conditions

Embankment slope	1 on 3.5 for all tests
W_{50}	34 gms for all tests
d	60 cm for all tests
T	0.89, 1.33, 1.80, 2.69, and 3.57 seconds

Table 3. Phase III Test Conditions

Embankment slope	1 on 3.5 with a 1 on 10 fronting slope for all tests.
W_{50}	34 gms for all tests.

Wave Conditions	T_p (seconds)	d
JONSWAP spectrum	1.45	60 cm
Kitaigorodskii spectrum	1.42, 1.20	60 cm
	1.80*, 1.48*	45 cm*
Monochromatic	1.46* and 1.21*	60 cm*

* Test conducted to suggest answers, no conclusions made because too few data points.

13. Regrade the filter layer and return to step 4.

Table 1 shows the conditions tested in the Phase One tests. Selected tests were replicated in order to show reproducibility of the test results. Test conditions repeated were generally those showing low riprap stability so that the worst conditions were given closer scrutiny.

Phase Two, Small-Scale Monochromatic Tests

The Phase Two and Three tests were conducted in CERC's 45.7-meter-long by 0.46-meter-wide by 0.91-meter-deep tank. The blade is driven by an electrohydraulic wave generator that can be controlled by a function generator or a computer signal. In the case of the Phase Two tests, where monochromatic waves were tested, the function generator was used to control the blade. For the Phase Three tests, where irregular waves were tested, a computer signal was used to control the blade.

The Phase Two tests replicated at a 1:10 geometric scale with Froude similarity the Phase One tests. Width of the small tank is one tenth that of the LWT and the distance from the toe of the embankment to the generator blade in the small tank was made one tenth of the distance in the LWT tests. In the small-scale test the wave period and wave height were varied; the embankment slope and median stone weight were held constant. The embankment slope tested for all of the Phase Two tests was 1:3.5 which was one of the slopes tested in the Phase One tests (see Figure 4). The median stone weight was 0.034 Kg which, at a 1:10-Froude scale, replicates a prototype weight of 34 Kg (one of the weights tested in the Phase One tests).

The core material was compacted sand with a median diameter of 0.2 milimeters. No attempt was made to model the core material used in Phase One; the core material was considered impermeable to wave penetration in all three phases. Filter material consisted of small gravel with a 3- to 8-millimeter diameter and a gradation that approximated that of the Phase One tests (see Figure 5). The riprap material was the same in all three phases (a diorite with a specific gravity of 2.71). The shape of the riprap approximated that of the Phase One being generally blocky to angular in shape. Riprap gradation in the three phases was also the same,

$$\frac{1}{8} W_{50} \leq W \leq 4\ W_{50} \qquad \text{(Eq. 10)}$$

(see Figure 6). Gradations by weight of the riprap were measured throughout

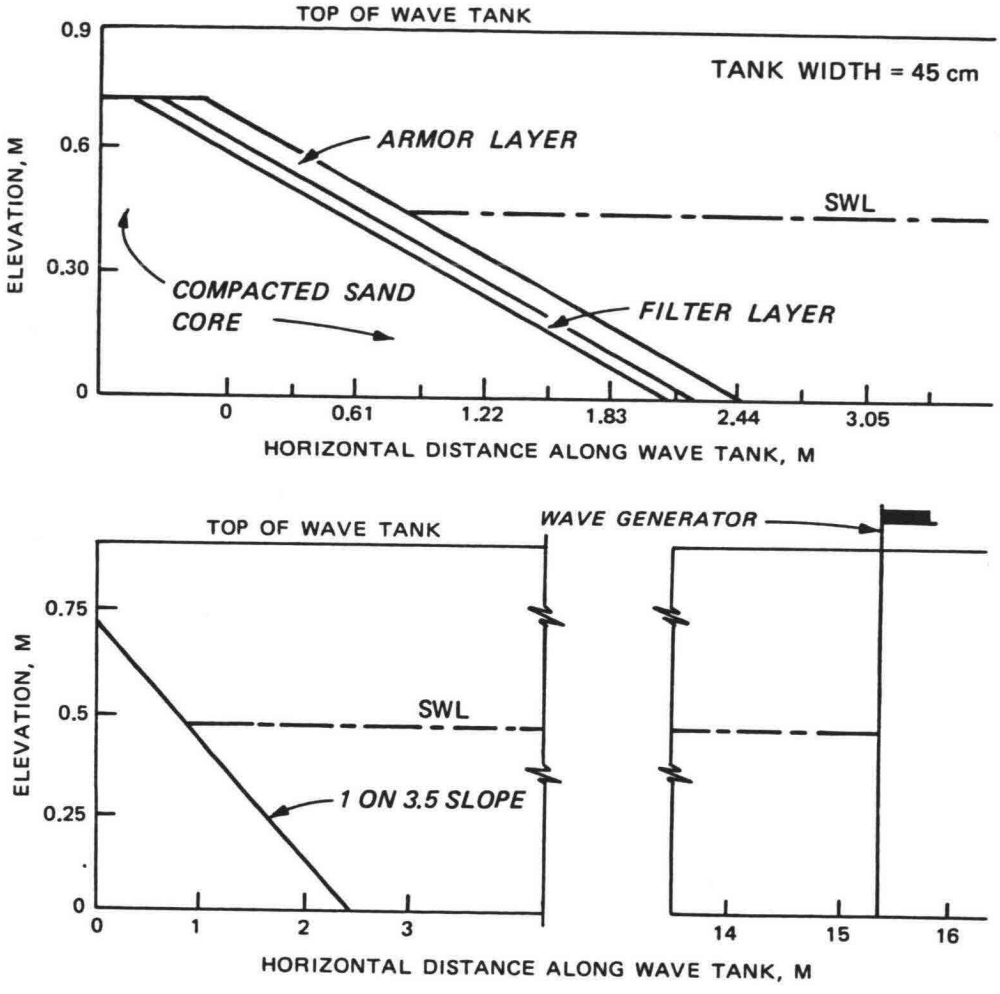

Figure 4. Phase Two Test Setup

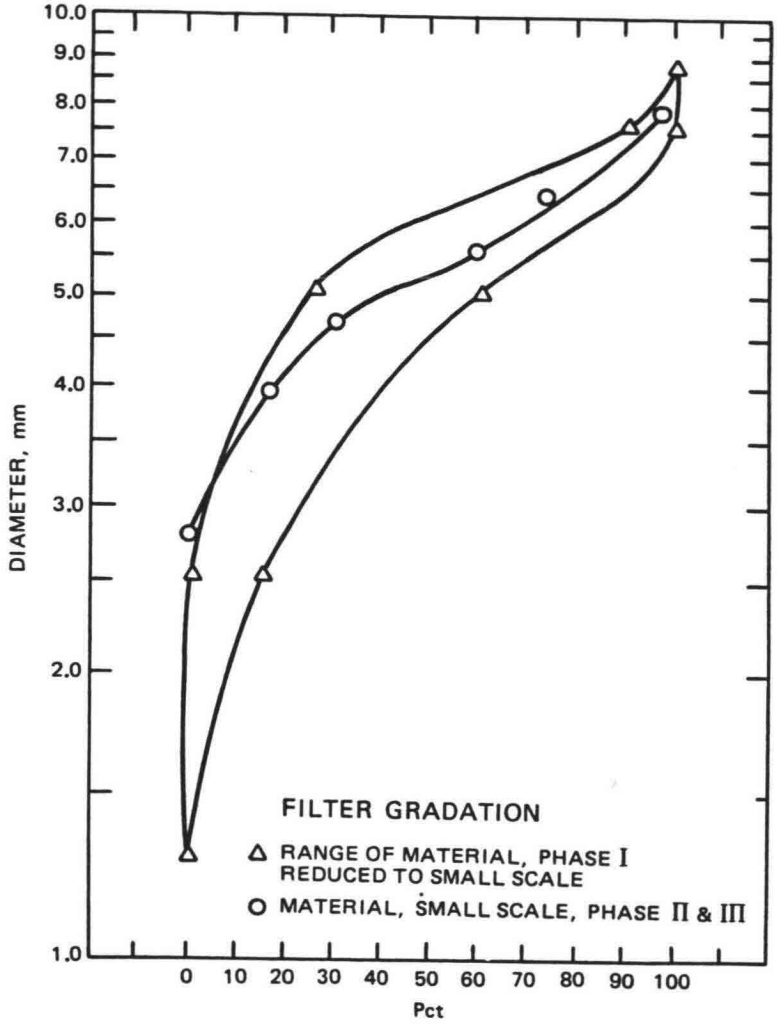

Figure 5. Filter Gradation

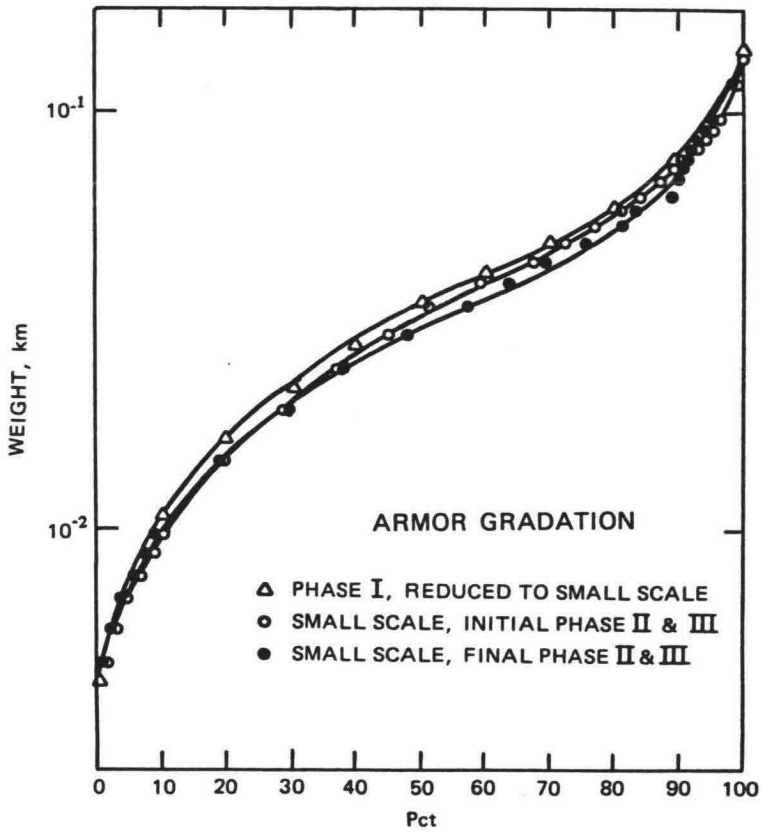

Figure 6. Armor Gradation

the study to ensure that the riprap in the small-scale tests modeled that of the large-scale tests.

Waves were run in bursts similar to the Phase One tests. The duration of the wave bursts, W_d , was equal to:

$$W_d = \frac{2S}{Cg} \qquad \text{(Eq. 11)}$$

where S is the distance from the toe of the embankment to the blade and Cg is the group celerity of the waves. During the Phase One tests the wave heights were measured prior to the construction of the embankment. In the Phase Two study the wave heights were measured while conducting the stability tests. Wave heights were recorded on two strip charts attached to two resistance gages placed a quarter of a wave length apart. Gages were placed close to the blade in order to maximize the number of waves recorded on the strip chart before re--reflected energy returned to the gages. The wave height was taken as the average of the wave heights from each of the two gages.

The following is the test procedure used during the Phase Two tests, which is similar to that of Phase One:

1. Place and compact core material;
2. Survey surface profile of the core;
3. Place and smooth filter layer;
4. Survey surface profile of the filter;
5. Place riprap stone by dumping from a hand-held container to simulate the prototype procedure of dumping from a skip;
6. Survey surface profile of the riprap (reference survey);
7. Run a series of wave bursts (same wave height and period) until no further stone movement is detected;
8. Survey surface profile of the riprap;
9. Increase the wave height approximately 10 percent and repeat Steps 7, 8, and 9;
10. Repeat Steps 7, 8, and 9 until failure is obtained; failure is defined as when enough riprap is shifted to expose the filter material;
11. Survey surface profile of the riprap;
12. Remove the riprap material and survey the damage filter layer;
13. Regrade the filter layer and return to Step 4 for the next test.

Table 2 shows the conditions tested during the Phase Two tests.

Phase Three, Small-Scale Irregular Tests

The Phase Three tests were conducted in the same wave tank and conducted using the same materials (core, filter, and riprap) as the Phase Two tests. The physical setup of Phases Two and Three was different (see Figures 4 and 7). The 1-on-30 fronting slope in the Phase Three tests was to allow the waves to shoal up the beach face as they would in a natural setting. Monochromatic waves also were run on the Phase Three setup so comparisons could be made between Phases Two and Three monochromatic wave tests and between Phase Three irregular and monochromatic wave tests. The only embankment slope tested in Phase Three was a 1:3.5 slope.

In Phase Three the laboratory computer was used to generate irregular waves. To use the computer to control the wave generator, a wave file had to be stored on magnetic tape. A wave file is a time history of blade displacements that the computer reads and sends to the generator. The transfer of the wave file from the computer to the generator is done through a digital-to-analog converter at a rate of 100 times a second.

The two wave spectra tested during Phase Three were the JONSWAP and Kitaigorodskii spectra. The JONSWAP (Joint North Sea Waves Project) spectrum is a deep-water wave spectrum that defines a growing sea state where the wave heights and wave periods are fetch-limited (Hasselmann, et al., 1973). The Kitaigorodskii spectrum is a wave spectrum that provides the highest wave conditions that could exist for a given frequency in a finite depth of water (Vincent, 1981). The basis for the spectrum is an equation derived by Kitaigorodskii, Karasitskii, and Zaslavski (1975) which defines the maximum energy density that can exist in a frequency component of a wave spectrum in a finite depth of water. These two spectra were chosen because they represent the conditions most likely to occur at a revetment site.

Wave heights were varied by using a potentiometer on the generator. The potentiometer had a range of 0 (no signal being transmitted to the generator) to 1.0 (full signal being transmitted to the generator). With the potentiometer set at 0.6 the generator received 60 percent of the full signal. Changing the potentiometer adjusted the amplitude of the blade motion but not the frequency of the motion. Thus, the significant wave height could be increased or decreased while the period of peak energy density and the relative wave height distribution (normalized by the mean wave height) remained the same.

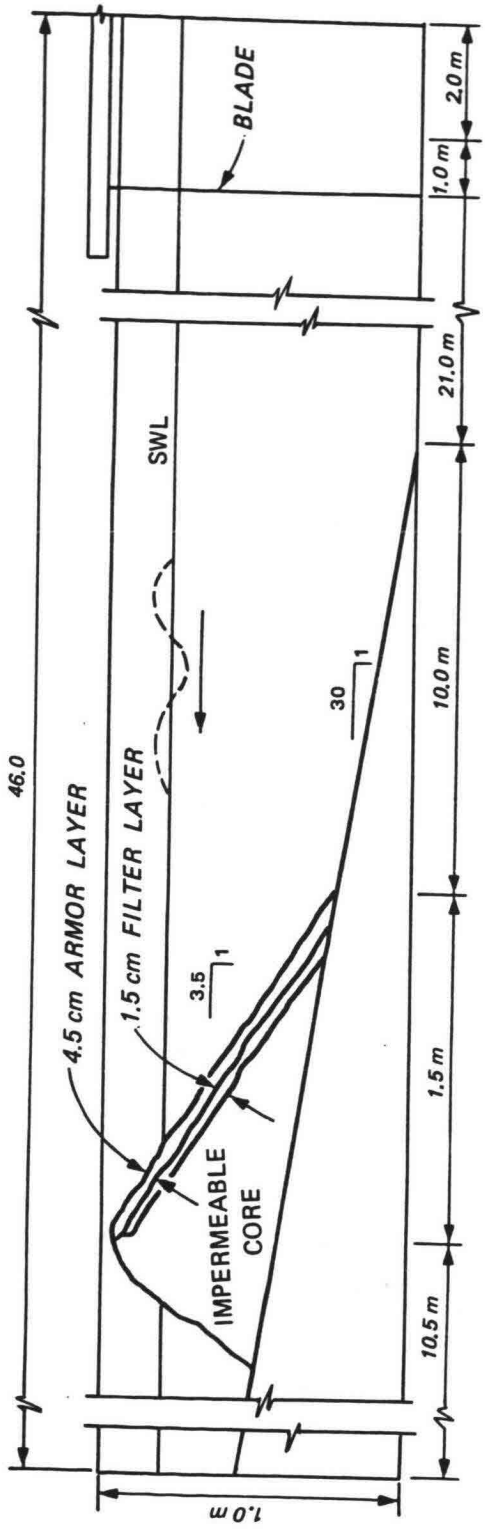

Figure 7. Phase Three Test Setup

The computer also was used to record and analyze the wave conditions that existed during a test. Wave data were collected by three parallel wire-resistance staff gages located at 20.1 meters, 20.4 meters, and 21.0 meters from the blade. Gages were calibrated before and after each test and wave records were collected several times during a test. Each wave record was sampled at a rate of 16 times a second for 260 seconds.

The test procedures for the Phase Three tests were different than the procedures followed for Phases One and Two and were as follows:

1. Place, compact, and survey surface profile of the core;
2. Place, smooth, and survey surface profile of the filter;
3. Place riprap stone by dumping from a hand-held container to simulate the prototype procedure of dumping from a skip;
4. Survey surface profile of the riprap (reference survey);
5. Generate waves for one hour;
6. Survey surface profile of the riprap;
7. Repeat steps 5 and 6 until failure or stability; failure is defined as when enough riprap material has shifted to expose the filter material, and stability is defined as when negligible change occurs to the surface profile (approximately 5000 waves);
8. Remove the riprap material and survey the damage filter layer;
9. Regrade and survey the filter material and return to step 3 for the next test.

Table 3 shows the conditions tested during the Phase Three study.

Survey Device for All Three Phases

The apparatus used to survey the embankment slope consisted of six vertical sounding rods mounted on a rack moving along level rails fixed on top of the tank walls. A circular foot was attached to the end of each survey rod by a ball-and-socket joint. In Phase One the circular foot was 15 centimeters in diameter and for Phases Two and Three the circular foot was 1.8 centimeters in diameter, approximately one tenth of the Phase One foot diameter. The surface elevations were measured over a square grid in a horizontal plane. For Phase One the points were 0.61-by-0.61-meters apart and for Phases Two and Three the points were 0.06-by-0.06-meters apart.

Method of Data Analysis

Damage to the riprap armor layer is quantified by comparing the profile of the riprap armor layer taken after wave attack (damage profile) to the profile taken before any wave attack (reference profile). The comparison is shown schematically in Figure 8. The damage profile typically consists of an erosion zone and an accretion zone. The volume per unit length (across the tank) of the erosion zone was used to quantify the damage, D. The damage, D, was made dimensionless, D', by dividing by the cube-root squared of the median stone weight, W_{50}, divided by the unit weight of riprap, ω_r (2707 kg/m^3).

$$D' = \frac{D}{\left(\frac{W_{50}}{\gamma_r}\right)^{2/3}} \qquad \text{(Eq. 12)}$$

The incident wave height was made dimensionless by using Hudson's (1958) stability number, N_s.

$$N_s = \frac{H}{\left(\frac{W_{50}}{\omega_r}\right)^{1/3}\left(\frac{\gamma_r}{\gamma_w} - 1\right)} \qquad \text{(Eq. 13)}$$

where γ_w is the unit weight of fresh water (1000 Kg/m^3). For Phases One and Two the modal wave height was used as the incident wave height (see discussion under Laboratory Setup for Phases One and Two). For Phase Three irregular waves, several wave heights were assumed for the incident wave height, i.e. significant and average of the highest 10 percent.

Figure 9 shows a data set for each of the three phases; Phase One SPL-19, Phase Two SET-1, Phase Three J#3. Figure 9 illustrates the typical damage trends observed. The data were fitted by curves of the form

$$D' = aN_s^{\,b} \qquad \text{(Eq. 14)}$$

where a and b are dimensionless coefficients. Shown on Figure 9 is the zero damage level, $D' = 2.0$, which is the lowest level of damage that can be consistently detected in the survey data. Curves of the form of Equation 14 were fitted to all the data (see Tables 4 and 5). Two parameters were selected to characterize the damage trend, N_z, the stability number that corresponds to the zero damage level, and b, the regression coefficient.

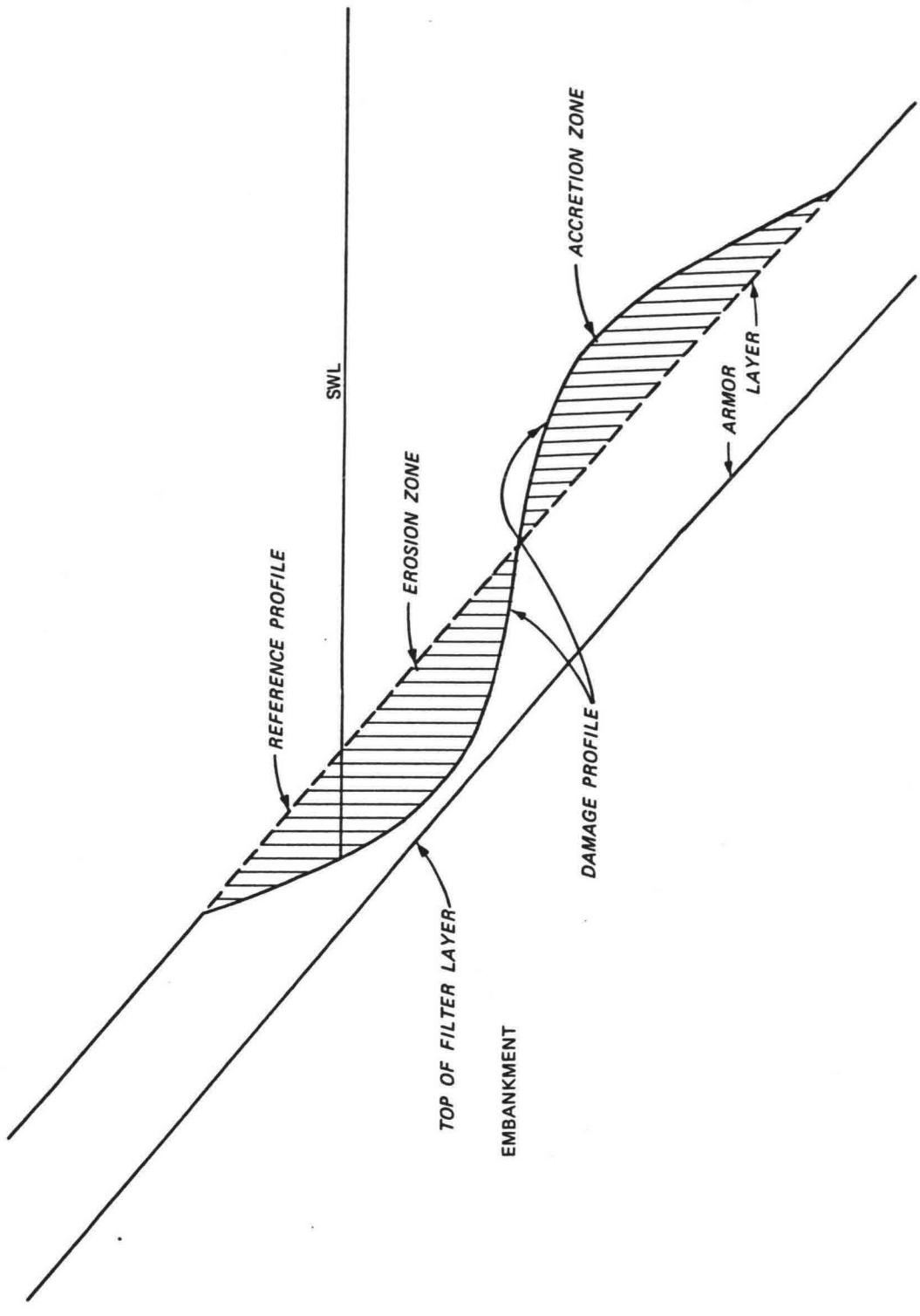

Figure 8. Typical Riprap Damage Profile

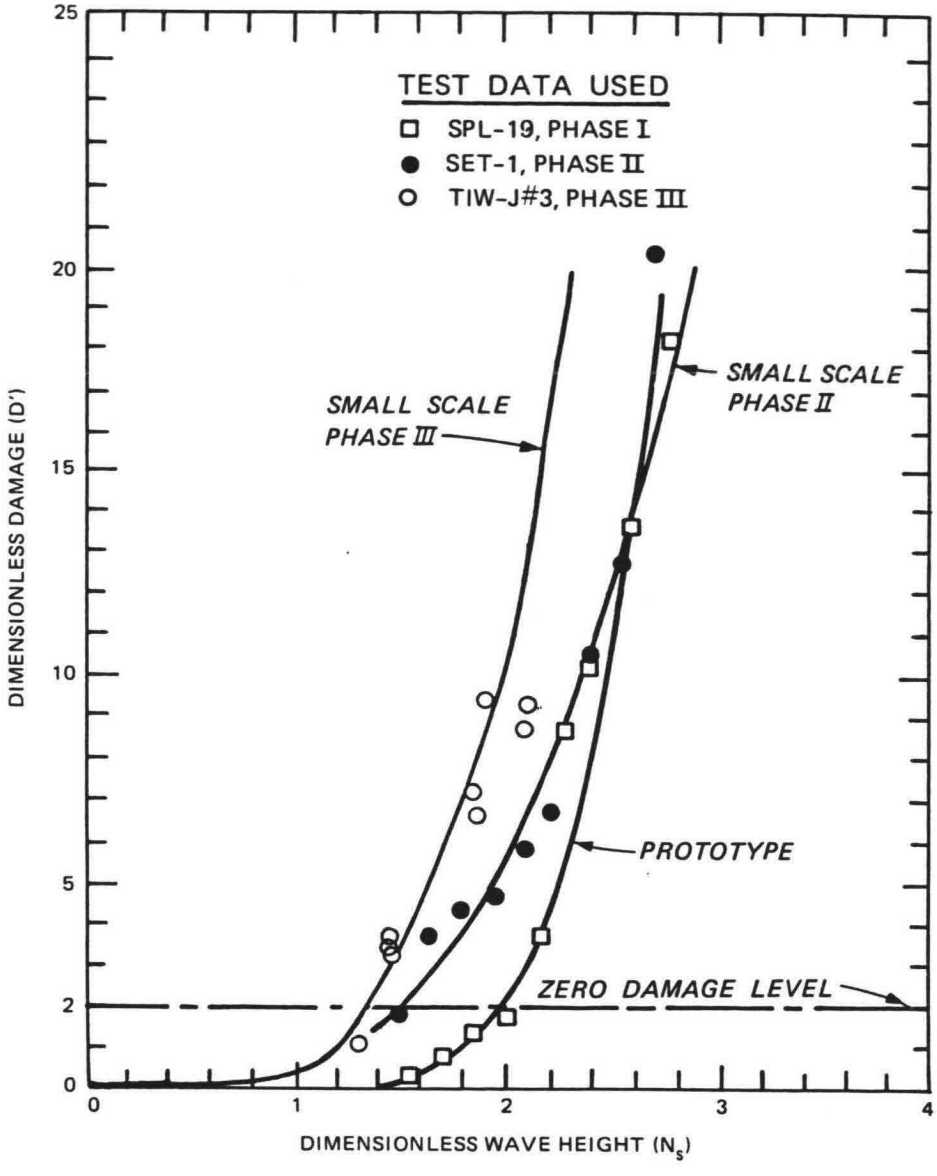

Figure 9. Typical Damage Trends

Table 4. Basic Data, Phases I and II

Test Designation[1]	d/gT^2	T (s)	Armor Layer Thickness (cm)	W_{50} (kg)	N_z	N_{zp}	b	H_z (cm)
SPL-17	0.0595	2.80	41.76	34.02	2.834	2.648	6.333	112.56
SPL-27	0.0595	2.80	29.56	12.25	2.462	2.648	5.151	69.56
SET-7	0.0588	0.89	5.12	0.034	1.870	-----	3.410	7.44
SET-8	0.0588	0.89	4.97	0.034	1.644	-----	2.210	6.52
SET-22	0.0588	0.89	4.97	0.034	2.267	-----	6.313	9.02
SET-24	0.0588	0.89	4.48	0.034	2.604	-----	5.694	10.33
SPL-18	0.0264	4.2	39.32	34.02	2.455	2.136	4.355	97.51
SPL-25	0.0264	4.2	52.43	34.02	2.185	2.136	5.969	86.78
SPL-28	0.0264	4.2	30.48	12.25	1.862	2.136	4.686	52.61
SPL-35	0.0264	4.2	55.47	54.43	2.042	2.136	3.736	94.85
SET-2	0.0264	1.33	5.40	0.034	1.816	-----	3.591	7.22
SET-4	0.0264	1.33	4.12	0.034	1.772	-----	3.902	7.04
SET-9	0.0264	1.33	5.03	0.034	1.610	-----	3.310	6.40
SET-19	0.0264	1.33	5.55	0.034	1.431	-----	2.844	5.67
SPL-19	0.0144	5.7	46.33	34.02	1.979	1.970	7.149	78.61
SPL-23	0.0144	5.7	44.81	34.02	1.803	1.970	5.179	71.60
SPL-29	0.0144	5.7	29.87	12.25	1.780	1.970	6.841	50.29
SPL-32	0.0144	5.7	42.37	54.43	2.359	1.970	8.206	109.58
SPL-36	0.0144	5.7	42.06	54.43	1.928	1.970	6.120	89.55
SET-1	0.0144	1.80	4.78	0.034	1.490	-----	3.512	5.88
SET-3	0.0144	1.80	4.51	0.034	1.412	-----	4.709	5.61
SET-10	0.0144	1.80	5.06	0.034	1.605	-----	5.682	6.37
SET-20	0.0144	1.80	4.82	0.034	1.624	-----	4.083	6.46
SPL-20	0.00646	8.5	43.89	34.02	2.051	2.059	7.614	81.47
SPL-24	0.00646	8.5	46.63	34.02	2.020	2.059	6.611	80.22
SPL-30	0.00646	8.5	25.91	12.25	2.165	2.059	12.195	61.17
SPL-33	0.00646	8.5	45.72	54.43	2.102	2.059	7.573	97.66
SPL-37	0.00646	8.5	51.51	54.43	1.959	2.059	5.396	91.01
SET-5	0.00646	2.69	4.45	0.034	1.406	-----	2.422	5.58
SET-6	0.00646	2.69	4.36	0.034	1.829	-----	5.040	7.13
SET-11	0.00646	2.69	4.48	0.034	1.805	-----	4.856	7.16
SET-21	0.00646	2.69	4.54	0.034	1.802	-----	4.705	7.16
SPL-22	0.00365	11.3	47.24	34.02	2.387	2.370	8.145	94.79
SPL-31	0.00365	11.3	29.26	12.25	2.235	2.370	6.687	63.15
SPL-34	0.00365	11.3	48.46	54.43	2.487	2.370	8.480	115.52
SET-12	0.00366	3.57	3.84	0.034	1.694	-----	7.000	6.64
SET-13	0.00366	3.57	4.18	0.034	1.649	-----	5.525	6.55
SET-23	0.00366	3.57	4.82	0.034	1.996	-----	8.479	7.92

[1]SPL: Phase I LWT test; SET: Phase II small-scale test.

Table 5. Basic Data Phase III

	J#3	V#1	V#2
d, depth of water	60 cm	60 cm	60 cm
W_{50}	34 gms	34 gms	34 gms
type of spectrum	JONSWAP	Kitaigorodski	Kitaigorodski
T_p	1.45 sec	1.42 sec	1.20 sec
range in H_s	4 cm - 10 cm	5 cm - 11 cm	3.5 cm - 10.5 cm
N_{sz} H_s	1.2440	1.3469	1.4435
b	3.5562	3.6617	3.7542
N_{mz} H_m	1.9996	2.2431	2.5619
b	3.5634	3.6561	4.5188
N_{05z} H_{05}	1.4929	1.6453	1.7683
b	3.5629	3.6591	3.9300
N_{10z} H_{10}	1.2988	1.4261	1.5376
b	3.5624	3.6607	3.9156

$$N_z = \left(\frac{D_z'}{a}\right)^{1/b} = \left(\frac{2}{a}\right)^{1/b} \qquad \text{(Eq. 15)}$$

where $D_2' = 2.0$, the zero damage level. The regression coefficient, b , characterizes the rate of increase of damage with increasing wave height.

Results

Evaluation of Scale Effects

The values of N_z and b for the Phases One and Two tests are plotted versus the relative water depth in Figure 10 to demonstrate the influence of both the scale effects and the wave period on N_z and b . Figure 10 shows that the small-scale tests, Phase Two, had lower values of N_z and generally lower values of b than the prototype tests, Phase One. This indicates that damage is initiated earlier in the small-scale tests than in the prototype tests but proceeds at a slower rate with respect to increased wave height. The convergence in the damage trends typical of small-scale and prototype tests can be seen in Figure 9. In Figure 9 the regression curves cross; however, the actual data indicate that while the damage levels in the small-scale tests may approach those of the prototype, they do not surpass the prototype damage levels for similar values of dimensionless wave height, N_s . Figure 11 shows all the Phases One and Two data with a relative water depth, $d/gT^2 = 0.0144$, which includes the Phases One and Two data plotted in Figure 9. The small-scale and the prototype data fields overlap but do not cross as suggested by the regression curves. For the tests where the relative water depth was 0.0264 or 0.0065 there was more overlap or convergence of the small-scale and prototype data fields than shown in Figure 11. For tests where the relative water depth was 0.0037 there was no overlap and little convergence in the damage trends. The reason for the convergence in the damage trends is unclear, but may reflect a reduction of scale effects from the zero damage levels with the larger stability numbers (thus higher Reynolds number), the influence of breaker characteristics or the size of the data set and the inherent scatter in the data.

In evaluating scale effects between small-scale tests, Phase Two, and prototype scale tests, Phase One, the wave runup also was compared. Runup was observed visually and defined as the average point of maximum wave uprush in the riprap surface near the center line of the slope. The elevation of this point (maximum wave uprush) then was measured using the survey device. Runup,

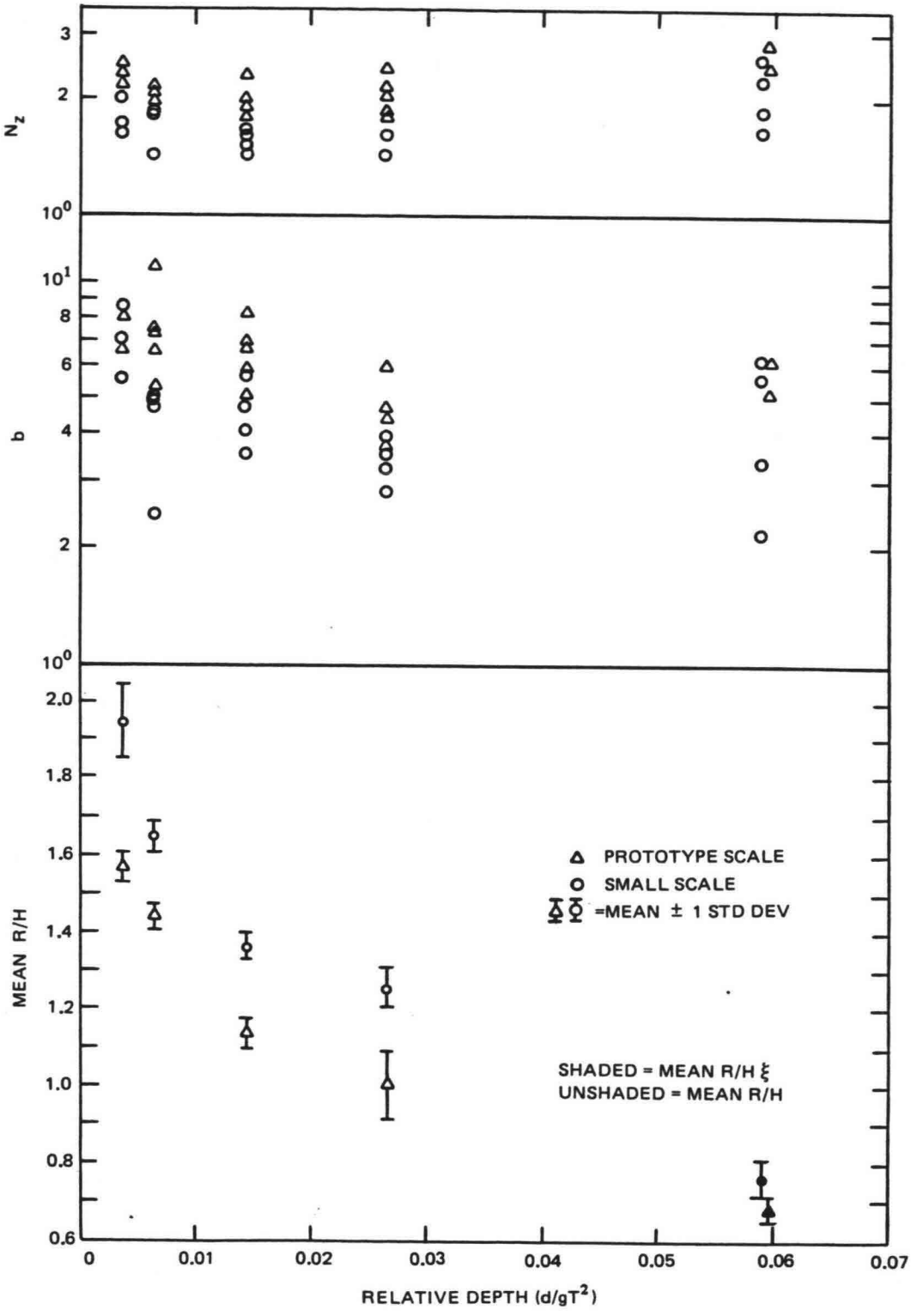

Figure 10. Phases One and Two: Zero Damage Stability Numbers N_z, Damage Rate Coefficients b, and Relative Runup R/H, Versus Relative Depth

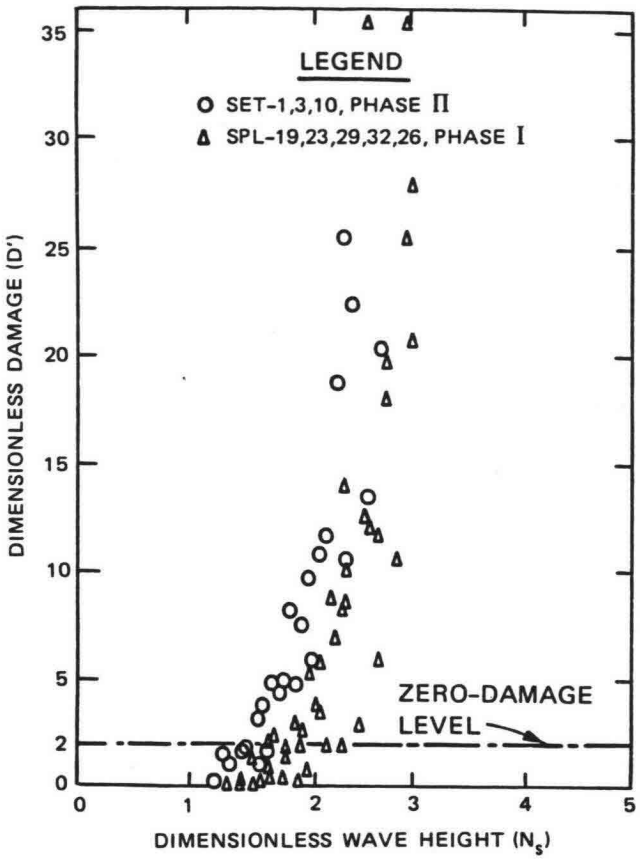

Figure 11. Phases One and Two Damage Trends $d/gT^2 = 0.0144$

R , was equal to the elevation of maximum wave uprush minus the elevation of the still water level. The runup in Table 6 indicates that a relative runup, R/H , can be considered constant for a fixed value of relative water depth between 0.0264 and 0.0036. For a relative water depth of 0.0595 or 0.0598, the ratio of the relative runup to the surf parameter, ξ , is almost constant, where

$$\xi = \left(\frac{H}{L_o}\right)^{-1/2} \tan \theta \qquad \text{(Eq. 16)}$$

where H is the wave height at the toe of the structure and L_o is the deep-water wave length. Runup invariants, R/H or $(R/H)/\xi$ (as tabulated in Table 6 and shown in Figure 10) indicate that the runup in the small-scale tests was approximately 20 percent greater than predicted from the prototype tests.

Scale Effects

When evaluating the results from the Phases One and Two tests, the small-scale tests give more conservative results than the prototype-scale tests at the zero damage levels. The stability numbers are lower and wave runup is higher in the small-scale tests. Higher runup is probably due to the reduced penetration of the wave uprush into the filter material. This indicates that the stone size used in the filter layer should be somewhat larger (than if the stone were scaled geometrically) to obtain proper flow similitude between small-scale and prototype-scale tests (Keulegan 1973).

Flow Regime

The small-scale tests, Phases Two and Three, replicated the prototype-scale tests, Phase One, at a 1:10 Froude scale. Assuming no scale effects requires rough turbulent flow in both the small-scale and prototype-scale tests. To check the existence or nonexistence of rough turbulent flow, criterion established by Jonsson (1966 & 1978) were used. Using definitions similar to Madsen and White (1976) who applied Jonsson's criterion to rubble-mound structures, the Reynolds number, R_E , is given by

$$R_E = \frac{R_z^2 \, (1 + \cot^2\theta) \, (\frac{2\pi}{T})}{\nu} \qquad \text{(Eq. 17)}$$

Table 6. Runup

Wave Period, T (s)	d/gT^2	R/H		$\frac{R/H}{\xi}$		N	Std. Dev. / Mean
		Mean	Std. Dev.	Mean	Std. Dev		
2.89	0.0595	-----	-----	0.682	0.024	7	0.035
0.89	0.0588	-----	-----	0.760	0.051	18	0.067
4.20	0.0264	1.004	0.086	-----	-----	8	0.086
1.33	0.0264	1.257	0.050	-----	-----	4	0.040
5.7	0.0144	1.138	0.040	-----	-----	12	0.035
1.80	0.0144	1.366	0.033	-----	-----	5	0.024
8.5	0.0064	1.444	0.021	-----	-----	11	0.015
2.69	0.0064	1.649	0.040	-----	-----	6	0.024
11.3	0.0037	1.568	0.038	-----	-----	6	0.024
3.57	0.0037	1.948	0.097	-----	-----	13	0.050

and the roughness term, r_t , by

$$r_t = \frac{R_z(1+\cot^2\theta)^{1/2}}{\left(\frac{W_{50}}{\gamma_r}\right)^{1/3}} \qquad \text{(Eq. 18)}$$

where R_z is the wave runup associated with the zero damage wave height, H_z ; and ν is the kinematic viscosity. The values of runup used to compute the Reynolds number and roughness term are tabulated in Table 6 and represent the estimated runup which would be caused by the zero-damage wave height, H_z . H_z is calculated by using the value of N_z and Equation 13. Since the Reynolds number defined in Equation 17 uses wave runup, the Reynolds number refers to the flow regime at the surface of the riprap, not the conditions in the filter layer. In Figure 12 the Reynolds number and roughness values tabulated in Table 7 are shown with the flow regime boundaries. The figure shows that all three phases of the study are within the rough, turbulent flow regime.

Comparison of Scale Effects from this Study to Two Other Scale Effects Studies

The scale effects from this study were compared to two other scale effects studies (Dai and Kamel 1969, and Thomsen, Wohlt, and Harrison 1972) (see Figure 13). Dai and Kamel used rough quarrystone in their rubble-mound structure and Thomsen, Wholt, and Harrison used dumped Kimmswick limestone in their stability tests. The comparison was made by plotting the scale effects factor, $N_z/\bar{N}_{zp}$, versus the Reynolds number, R_n . The scale effects factor is the individual values of N_z divided by the average prototype value of N_z (designated $\bar{N}_{zp}$), values for this study are shown in Table 4. The Reynolds number is given by

$$R_N = \frac{\left(gH_z\right)^{1/2}\left(\frac{W_{50}}{\gamma_r}\right)^{1/3}}{\nu} \qquad \text{(Eq. 19)}$$

the kinematic viscosity, ν , is assumed equal to 1.130×10^{-6} meters-squared per second which corresponds to a water temperature of 15.6 degrees Celsius. Figure 13 shows that at the zero-damage level the scale effects observed in this study were somewhat less severe than those observed by Thomsen, Wholt, and Harrison and more severe than those observed by Dai and Kamel.

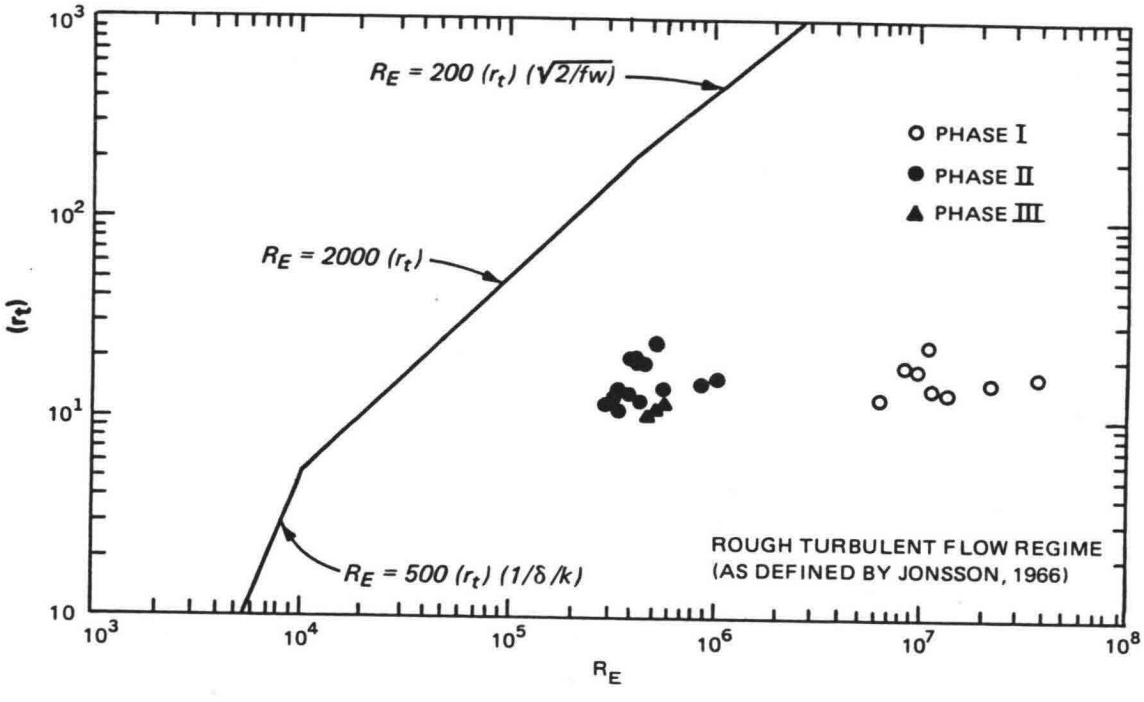

Figure 12. Flow Regime

Table 7. Flow Regime Computations[1]

Test Designation	d/gT^2	T	W_{50}	ν 1×10^{-5}	k [2]	R_z	a_{im}/k (Eq. 6)	R_e 1×10^{-5} (Eq. 5)
SPL-17	0.0595	2.8	75.0	0.97	0.763	3.48	16.60	371.0
SET-22	0.0588	0.89	0.075	1.06	0.0763	0.313	14.94	8.65
SET-24	0.0588	0.89	0.075	1.02	0.0763	0.335	15.98	10.29
SPL-18	0.0264	4.2	75.0	0.92	0.763	3.21	15.32	222.0
SPL-25	0.0264	4.2	75.0	1.20	0.763	2.86	13.64	135.0
SET-2	0.0264	1.33	0.075	0.99[3]	0.0763	0.300	14.33	5.71
SET-9	0.0264	1.33	0.075	1.00[3]	0.0763	0.264	12.59	4.36
SET-19	0.0264	1.33	0.075	1.00[3]	0.0763	0.234	11.15	3.42
SPL-19	0.0144	5.7	75.0	1.08	0.763	2.93	14.00	116.0
SPL-23	0.0144	5.7	75.0	1.50[3]	0.763	2.67	12.75	63.0
SET-1	0.0144	1.80	0.075	1.00[3]	0.0763	0.264	12.58	3.21
SET-3	0.0144	1.80	0.075	1.01[3]	0.0763	0.251	11.93	2.89
SET-10	0.0144	1.80	0.075	1.00[3]	0.0763	0.286	13.62	3.77
SET-20	0.0144	1.80	0.075	1.13	0.0763	0.291	13.82	3.43
SPL-20	0.00646	8.5	75.0	1.75	0.763	3.86	18.41	83.0
SPL-24	0.00646	8.5	75.0	1.48	0.763	3.80	18.13	96.0
SET-6	0.00646	2.69	0.075	1.06[3]	0.0763	0.386	18.41	4.35
SET-11	0.00646	2.69	0.075	1.00[3]	0.0763	0.388	18.49	4.65
SET-21	0.00646	2.69	0.075	1.12	0.0763	0.388	18.49	4.15
SPL-22	0.00365	11.3	75.0	1.59[3]	0.763	4.87	23.26	110.0
SET-12	0.00366	3.57	0.075	1.00[3]	0.0763	0.425	20.26	4.21
SET-13	0.00366	3.57	0.075	1.00[3]	0.0763	0.419	19.98	4.09
SET-23	0.00366	3.57	0.075	1.03	0.0763	0.506	24.16	5.21
J #3	0.0291	1.45	0.075	1.00[3]	0.0763	0.285	13.60	4.66
V #1	0.0303	1.42	0.075	1.00[3]	0.0763	0.230	10.97	3.10
V #2	0.0425	1.20	0.075	1.00[3]	0.0763	0.248	11.83	4.26

[1] All test $\cot\theta = 3.5$.

[2] $k = (W_{50}/\gamma_r)^{1/3}$.

[3] Assumed value of kinematic viscosity.

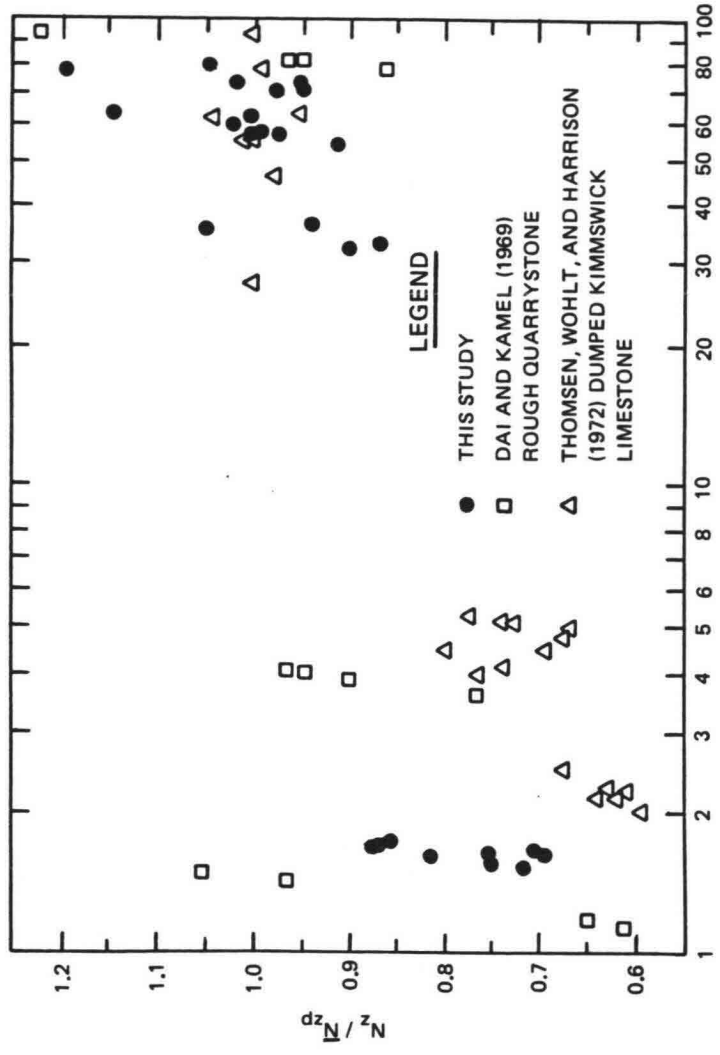

Figure 13. Scale Effects for Three Studies

Irregular and Monochromatic Waves

The data for the Phase Three study (small-scale with irregular waves) is tabulated in Table 5. The Phase Three stability data are plotted in Figure 14. Also in Figure 14 is the Phase Two stability data with a wave period of 1.8 seconds. The 1.8-second data were chosen because they gave the worst damage trends for the Phase Two tests (worst damage trends meaning that more damage would occur for a given wave height). In Figure 14 the significant wave height is the incident wave height used in the calculation of N_s for the Phase Three data. From Figure 14 it appears that the significant wave height is not the wave height parameter to use to compare monochromatic waves to irregular waves. When the significant wave height is used to estimate the amount of damage (for irregular waves), the estimate would be too low if the damage trends were established from small-scale monochromatic wave tests.

The damage trends for J#3 and V#1 are plotted in Figures 15 and 16, respectively. Several wave height parameters were used to calculate the stability number. The wave height parameters are: H_m, the maximum wave height; $H_{.05}$, the 5 percent wave height; $H_{.10}$, the 10 percent wave height; and H_s, the significant wave height. The monochromatic wave data, $T = 1.80$ seconds, also is plotted in Figures 15 and 16. From Figures 15 and 16 $H_{.10}$ or $H_{.05}$ should be the wave height parameter used to predict a similar amount of damage that would occur from monochromatic waves.

Several tests were run to verify that the difference between the physical setup of Phases Two and Three would not change the damage trends established during the Phase Two tests. Figure 17 shows that the monochromatic wave tests conducted on the Phase Three setup and three of the Phase Two damage trends. New monochromatic wave damage trends should have been established on the Phase Three setup (the 1-on-30 fronting slope) but time did not permit.

Phase Three Compared to Two Other Irregular Wave Studies

Phase Three results were compared to two other studies (Hydraulic Research Station, Wallingford, 1975, and Ahrens and Zirkle, 1982) that were conducted with irregular waves. The Wallingford tests were riprap stability tests conducted in deep water with the following variables: three sizes of

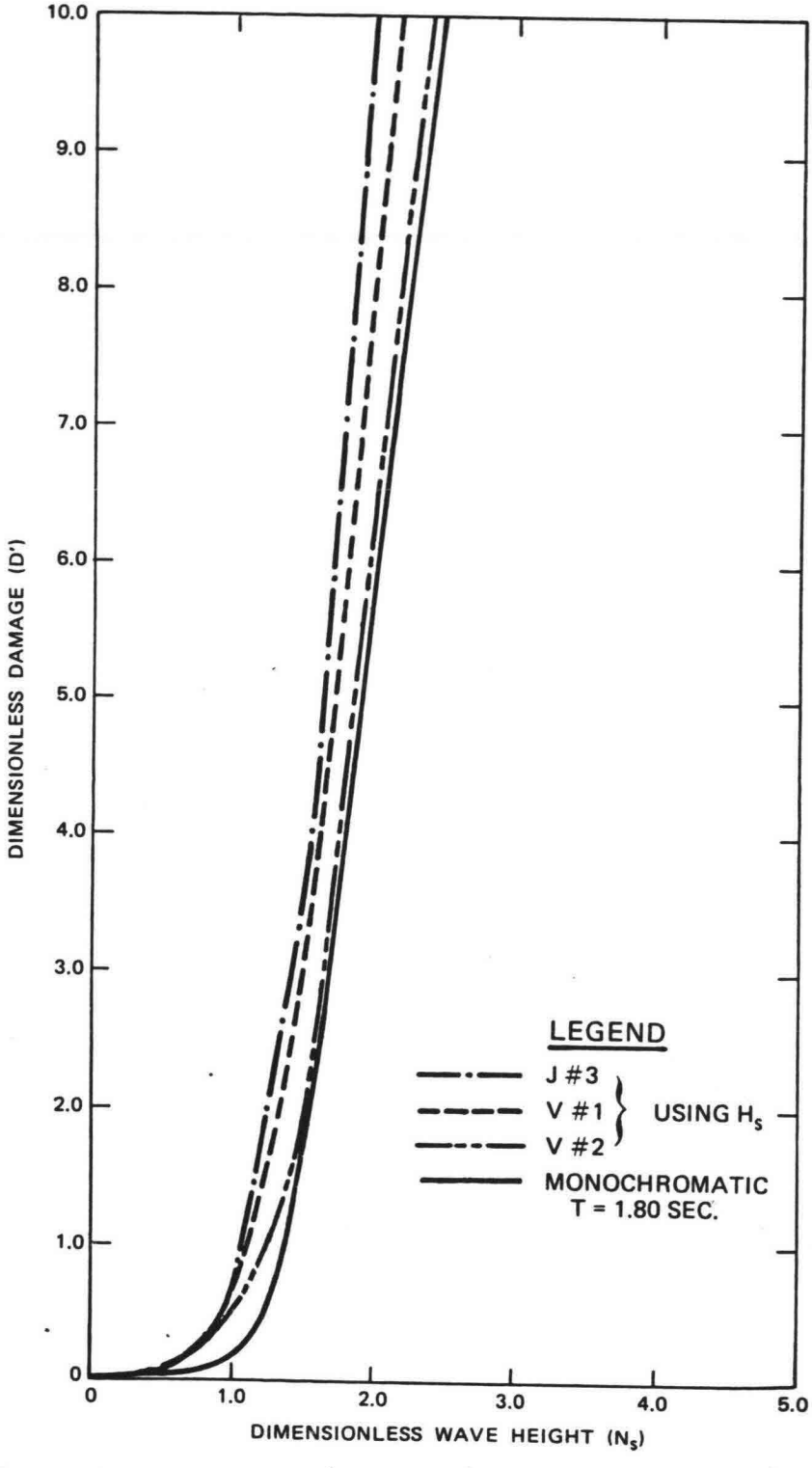

Figure 14. Irregular and Monochromatic Damage Trends

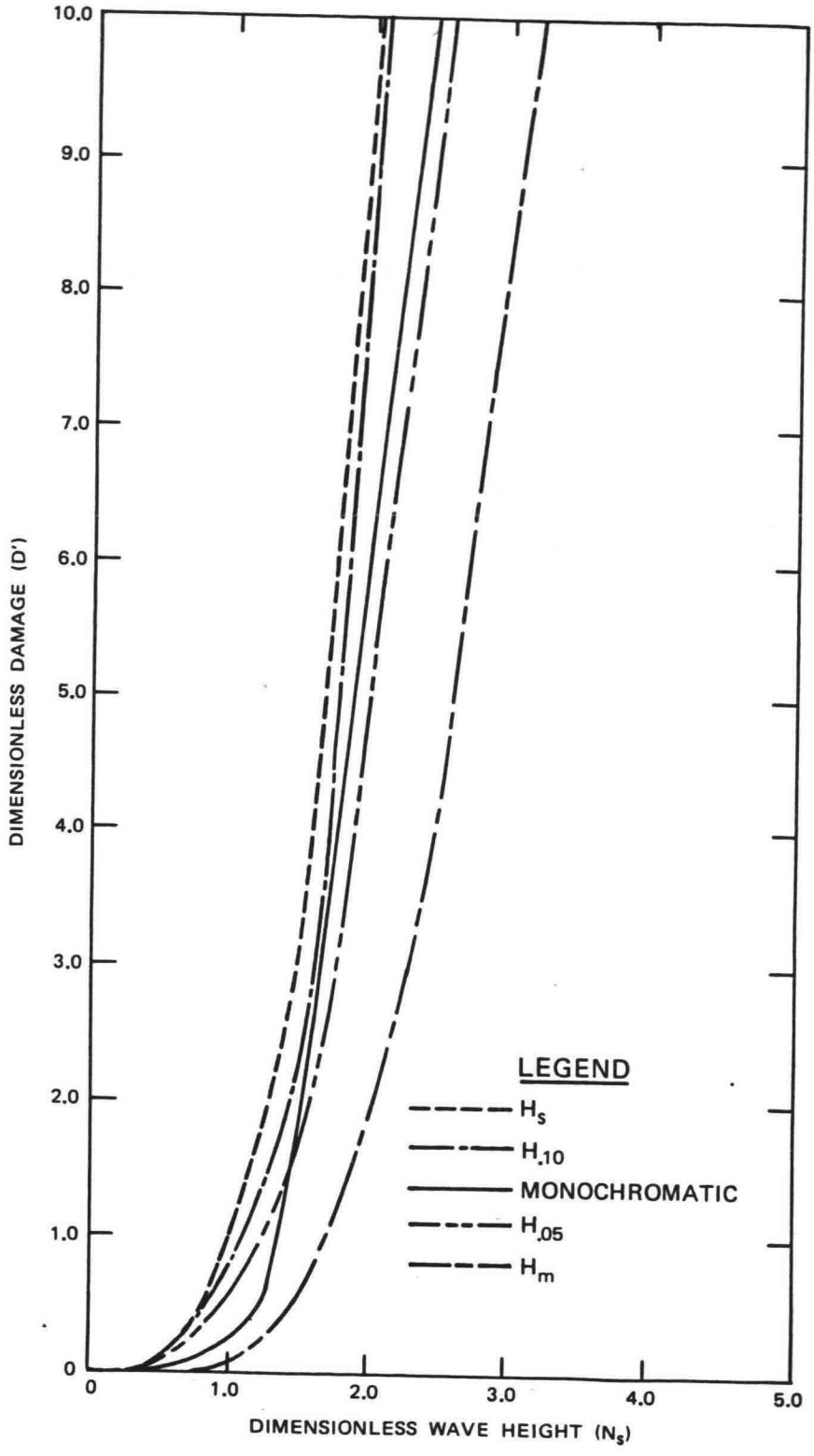

Figure 15. Damage Trends J#3, H_s, H_m, $H_{.10}$, and $H_{.05}$

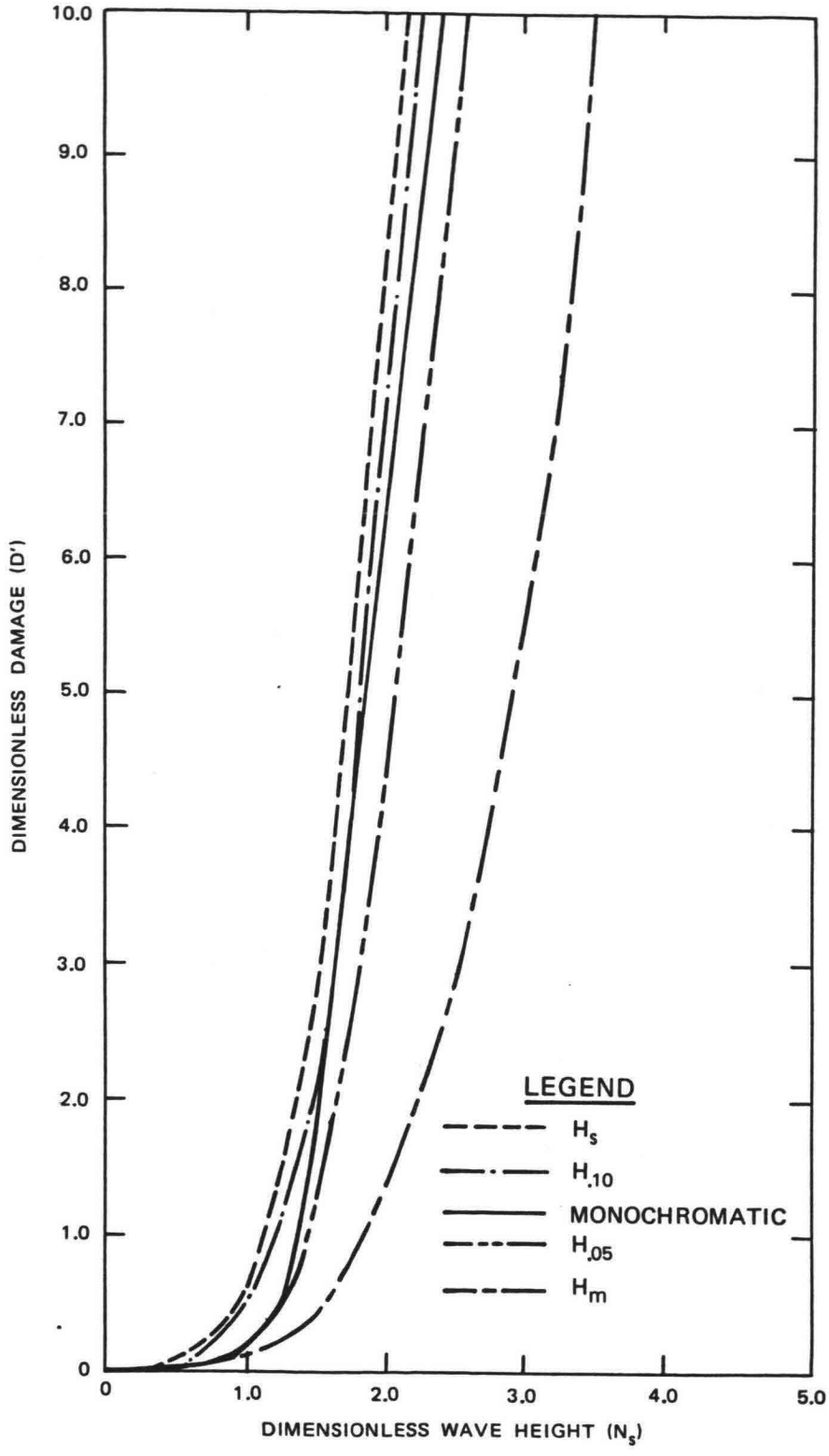

Figure 16. Damage Trends V#1, H_s , H_m , $H_{.10}$, and $H_{.05}$

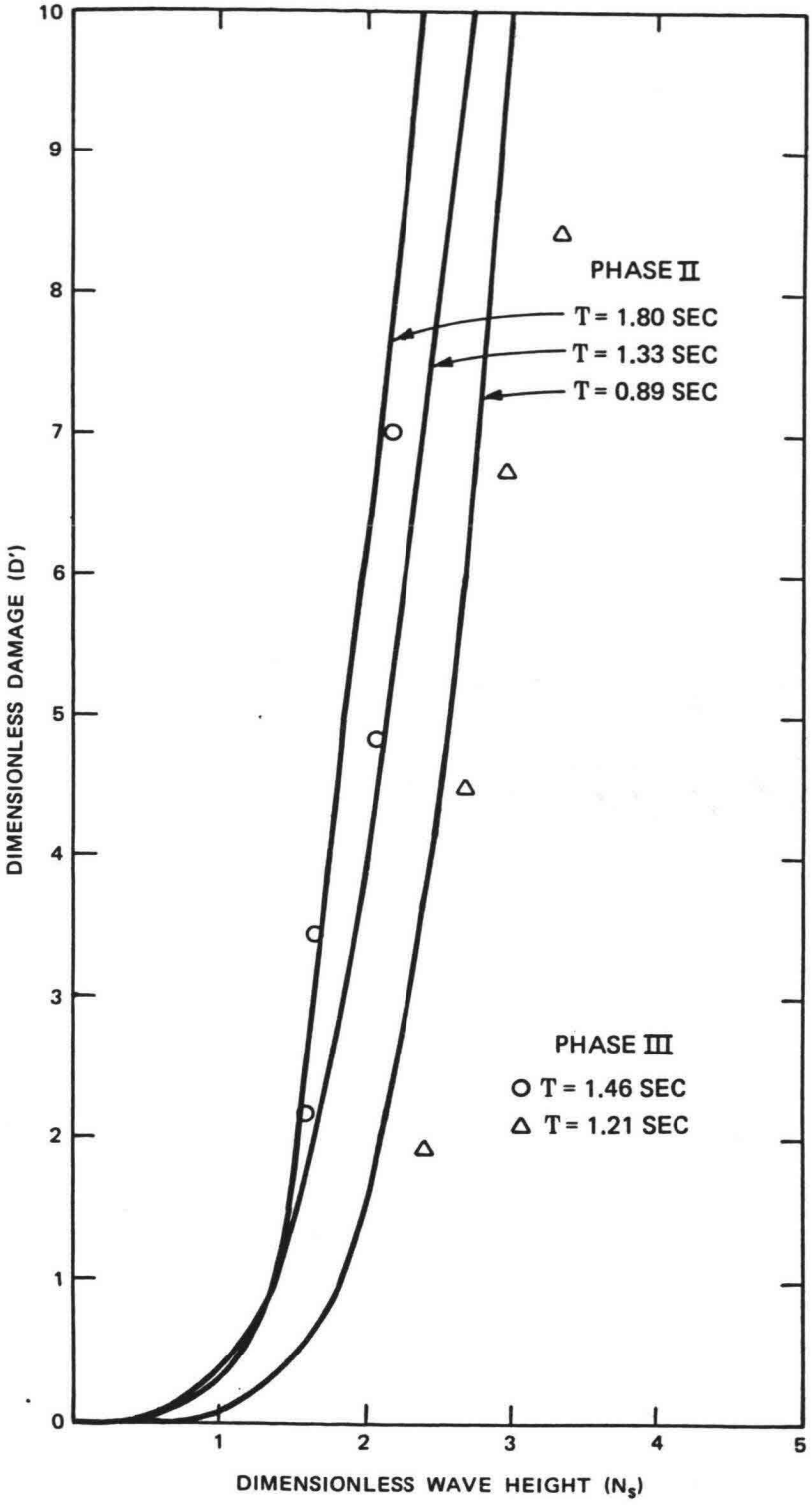

Figure 17. Monochromatic Wave Verification Test

riprap; JONSWAP spectrum with three mean wave periods (0.92, 1.13, and 1.30 seconds), each with several significant wave heights; and revetment slopes of 1 on 2, 1 on 3, 1 on 4, and 1 on 6. The Wallingford data with a mean riprap diameter, D_{50} equal to 3 cm, a revetment slope of 1 on 3, and a wave period of 1.30 seconds was used to compare to the Phase Three data. The D_{50} of 3 cm and a wave period of 1.30 seconds best approximated the conditions tested in Phase Three. The Ahrens and Zirkle tests were site-specific tests of riprap stability on Lake Okeechobee, Florida. The test structure was a 1-on-3 slope with a 1-on-12 fronting slope, the riprap had a W_{50} of 67 grams, and a Kitaigorodskii spectrum with a peak period of energy density was 1.45 seconds. In both the Wallingford tests and the Ahrens and Zirkle tests the revetment slope used for comparison is 1-on-3. This was chosen because this slope should have lower stability than the 1-on-3.5 slope of this study.

In Figure 18 the damage trends for the three studies are shown (see Table 8). The stability number for all three studies was calculated using H_s. For both the Wallingford and Ahrens and Zirkle tests the data plotted had a revetment slope of 1-on-3. The difference in the damage trends is probably due to the difference in the water level at the toe of the structure, approximately 60 cm for the Wallingford and Phase Three data, and 24 cm for the Ahrens and Zirkle data. For the Ahrens and Zirkle tests the large waves would break as they moved onshore, maintaining a high significant wave height but reducing the difference between $H_{.10}$, $H_{.05}$, and H_m relative to H_s.

Phase Three Extrapolated to Prototype Scale

Looking at the Phases Two and Three data, monochromatic wave and irregular wave tests, it was concluded that $H_{.05}$ of the irregular wave train should be equivalent to the monochromatic wave height. From Phases One and Two, large- and small-scale tests, the small-scale tests were found to be approximately 20 percent more conservative than the large-scale tests at the zero-damage level. When extrapolating the Phase Three, small-scale irregular waves to prototype scale, the above two conclusions work against each other. Using the first conclusion the five percent wave height would be used during design computations. Ignoring the first conclusion and using the second conclusion, the wave height used for design computations (at the zero damage level) would be decreased by 20 percent. Combining the two conclusions the irregular wave height that

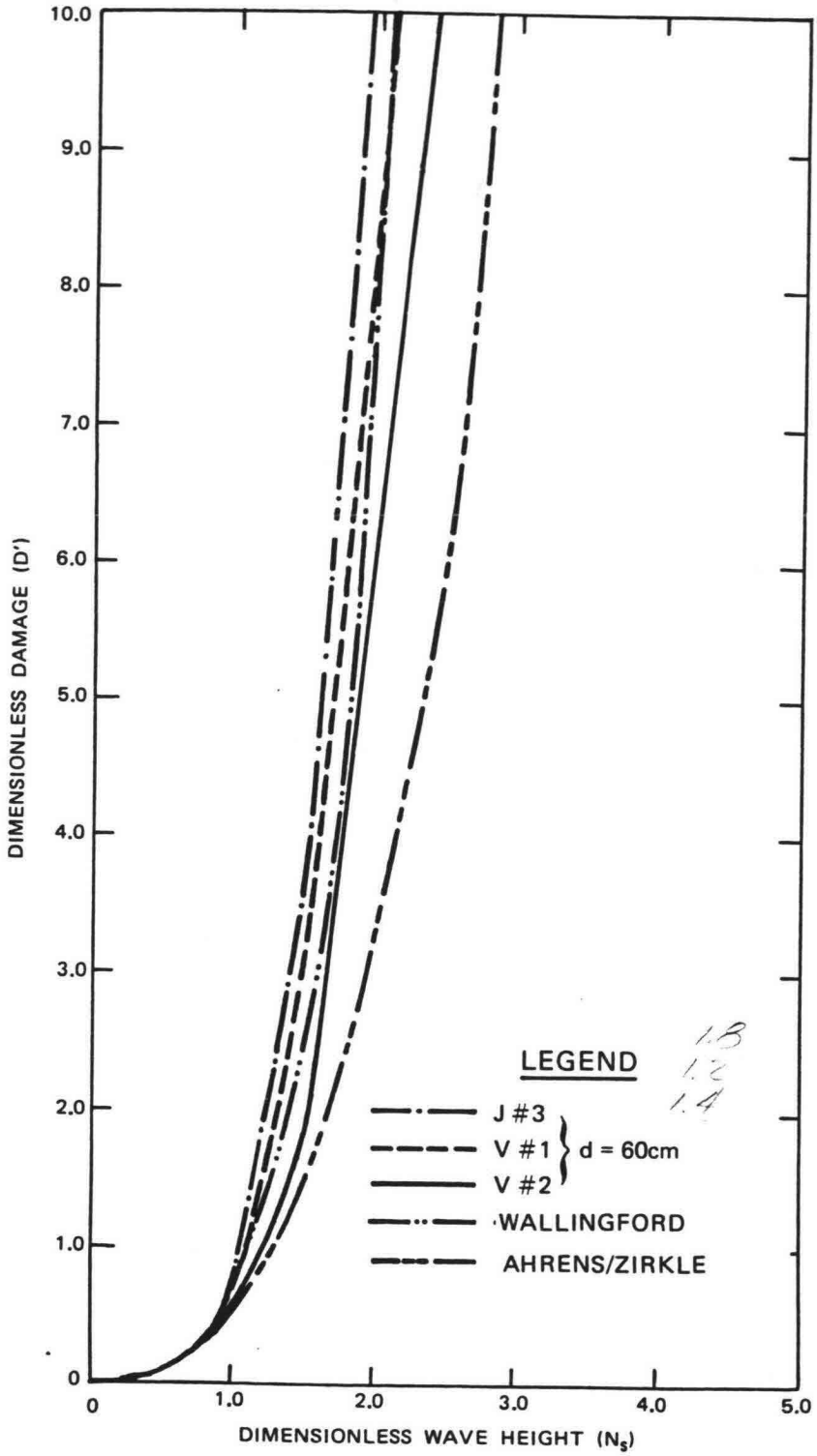

Figure 18. Damage trends and Water Depths for H

Table 8. Comparison with Other Data Sets

	J#3	V#1	V#2	Ahrens and Zirkle	Wallingford
d	60 cm	60 cm	60 cm	24 cm	61 cm
W_{50}	34 gms	34 gms	34 gms	67 gms	--
D_{50}	2.33 cm	2.33 cm	2.33 cm	--	3 cm
slope	1 on 3-1/2	1 on 3-1/2	1 on 3-1/2	1 on 3	1 on 3
N_{sz}	1.2440	1.3469	1.4435	1.5483	1.2689
b	3.5562	3.6617	3.9542	2.5695	3.486

should be used in design computation would be $H_{.05}$ reduced by 20 percent, which for the two spectra tested in Phase Three approximately would be H_s. Thus, in a prototype situation where the design guidance is based on small-scale monochromatic wave tests, the designer should use H_s when designing a revetment for stability at the zero-damage level.

Scale Effects Controversy

This three-phase study has concluded that scale effects exist but not of the magnitude defined by Thomsen, Wholt, and Harrison (1972). Thus, the question of the existence or nonexistence of scale effects has been answered, but why are there claims of no scale effects (Pitt and Ackers 1982), and why is the magnitude of the scale effects found by Thomsen, Wholt, and Harrison (1972) so large?

The explanation for the conclusions reached by Thomsen, Wholt, and Harrison (1972) can be explained by the data set. The results were derived from tests conducted for the U. S. Army Corps of Engineers, Missouri River Division (MRD), to solve site-specific riprap stability problems occurring on the large reservoirs in the Missouri Valley. Since this effort was not a basic research study, the scope was somewhat limited and time constraints forced compromises to be made during the course of testing. Therefore, although there is a large amount of MRD data, they are not ideal for evaluating scale effects. Ideally, to evaluate scale effects, there should be carefully paired tests between model and prototype in which the important dimensionless variables are replicated, as in Phases One and Two of this study. There are few matched pairs in the MRD data but all the data collected were grouped together to evaluate scale effects. As a result, the magnitude of the scale effects shown by Thomsen, Wholt, and Harrison includes other effects of undetermined magnitude and intensity.

An explanation as to why Pitt and Ackers (1982) claim that scale effects do not exist is conjectured at this point but by looking at some Wallingford data (1975) a possible explanation is as follows: the Wallingford data were compared to the Phase Two results (prior to Phase Three being conducted) and the two data sets showed approximately equal stability (Broderick and Ahrens 1982). This finding seemed to indicate that monochromatic and irregular wave tests would show about the same stability when the significant wave height was used to characterize the height of the irregular waves. However, when the

Wallingford data were compared to Phase Three, the Wallingford data showed slightly higher stability, Figure 18. When investigating this difference it was found that the ratio of the filter stone size to the armor stone size in the Wallingford tests was larger than that of this study. This would suggest that the Wallingford tests are relatively free of scale effects because of increased penetration of flow into the filter layer. Thus, a possible explanation is that the filter gradation relative to the armor gradation in the WASH study (Pitt and Ackers 1982) is larger than that of this study. If this is true, the WASH test would be relatively free of scale effects because of proper flow similitude in the filter layer.

Conclusions

A three-phase study on riprap stability was conducted to evaluate scale effects and monochromatic waves versus irregular waves (see Figure 19). Phase One was large-scale tests conducted using monochromatic waves. Phases Two and Three were small-scale tests with Phase Two using monochromatic waves and Phase Three using irregular waves.

Phases One and Two were compared and scale effects did exist. Small-scale tests were 20 percent more conservative than the large-scale tests at the zero-damage level. The scale effects are due to improper modeling of the flow regime in the filter layer. To overcome this the filter material should be scaled larger, but at this time no guidance exists as to how much larger the filter material should be.

When comparing Phases Two and Three, monochromatic waves and irregular waves, it was found that $H_{.05}$ or $H_{.10}$ (the five percent wave height or the 10 percent wave height) could be assumed equivalent to the monochromatic wave height. Ignoring scale effects, designers (when designing a revetment for stability) should use $H_{.05}$ or $H_{.10}$ in their computations. If the scale effects results are included the designer should use H_s when designing for the zero damage level. This assumes design guidance is based on small-scale monochromatic wave tests. The above conclusion stressed the zero-damage level because scale effects seem to be reduced as the stability numbers increased. Reduction in scale effects is seen in the convergences in the damage trends as the stability numbers increase (see Figure 9). The convergences of the damage trends seem reasonable because at higher stability numbers higher Reynolds numbers developed and viscous forces became less significant.

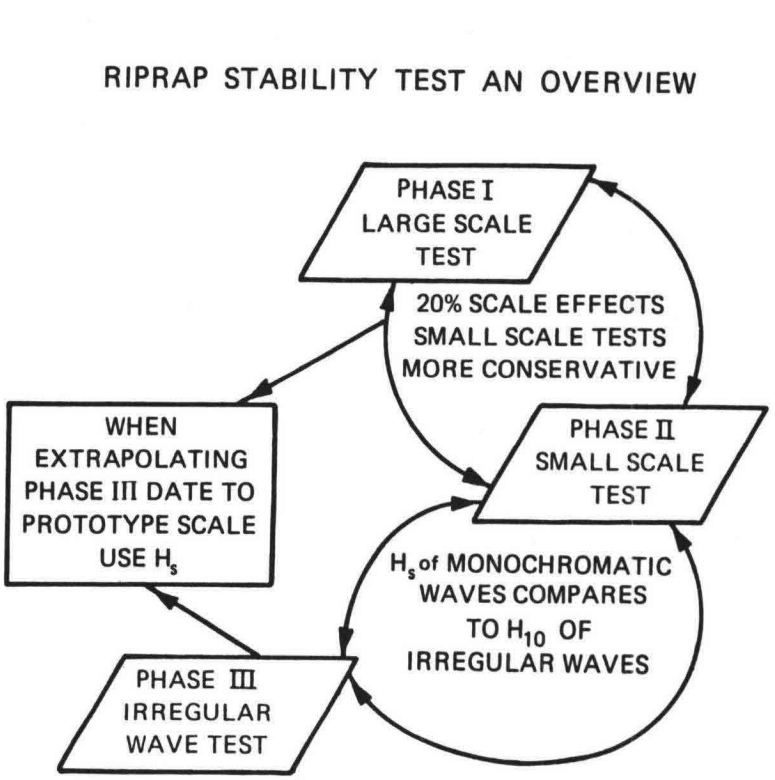

Figure 19. Riprap Stability Test, An Overview

References

Ahrens, J. P. "Large Wave Tank Tests of Riprap Stability." TM 51, U. S. Army Corps of Engineers, Coastal Engineering Research Center, Fort Belvoir, Virginia.

Ahrens, J. P., and Zirkle, K. P. "Riprap Stability Model Tests." unpublished report, U. S. Army Corps of Engineers, Coastal Engineering Research Center, Fort Belvoir, Virginia, June 1982.

Broderick, L. L., and Ahrens, J. P, "Riprap Stability Scale Effects." U. S. Army Corps of Engineers, Coastal Engineering Research Center. Technical Paper 82-3, Fort Belvoir, Virginia, August 1982.

Dai, Y. B., and Kamel, A. M. "Scale Effect Tests for Rubble-Mound Breakwaters." Research Report H-69-2, U. S. Army Engineer Waterways Experiment Station, Vicksburg, Mississippi, 1969.

Hasselmann, K., Barnett, T. P., Bouws, E., Carlso, H., Cartwright, D. C., Enke, K., Ewing, J., Gienapp, H., Hasselmann, D. E., Sell, W., Walden, H. "Measurements of Wind-Wave Growth and Swell Decay During the Joint Sea Wave Project (JONSWAP)," Deutshes Hydrographisches Institut, Hamburg, 1973.

Hudson, R. Y. "Design of Quarry-Stone Cover Layers for Rubble-Mound Breakwaters; Hydraulic Laboratory Investigation." Research Report 2-2, U. S. Army Engineer Waterways Experiment Station, Vicksburg, Mississippi, 1958.

Hudson, R. Y., Hermann, F. A., Jr. et al. "Coastal Hydraulic Models." U. S. Army Corps of Engineers, Coastal Engineering Research Center, Special Report 5, Fort Belvoir, Virginia, May 1979.

Hydraulic Research Station. "Riprap Design for Wind-Wave Attack, A Laboratory Study in Random Waves." Report No. EX 707, Wallingford, Oxfordshire, England, 1975.

Jonsson, I. G. "Wave Boundary Layers and Friction Factors." Proceedings of the 10th Conference on Coastal Engineering. American Society of Civil Engineers. 1966.

Jonsson, I. G. "A New Approach to Oscillatory Rough Turbulent Boundary Layers." Series Paper No. 17. Institute of Hydrodynamics and Hydraulic Engineering. Lyngby, Denmark. 1978.

Keulegan, G. H. "Wave Transmission Through Rock Structures; Hydraulic Model Investigation," Research Report H-73-1, U. S. Army Engineer Waterways Experiment Station. Vicksburg, Mississippi. June 1973.

Kitaigorodskii, S. A., Krasitskii, V. P., and Zasloaskii, M. M. "Phillips Theory of the Equilibrium Range in the Spectra of Wind-Generated Gravity Waves." Journal of Physical Oceanography. Vol. 5. 1975. pp. 410-420.

Madsen, O. S. "Waves Generated by a Piston-Type Wavemaker." Proceedings of the 12th Conference on Coastal Engineering. American Society of Civil Engineers. Vol. I. 1970. pp. 589-607. (Also Reprint 4-71. U. S. Army Corps of Engineers, Coastal Engineering Research Center, Fort Belvoir, Virginia. NTIS 732 607).

Madsen, O. S., and White, S. M. "Reflection and Transmission Characteristics of Porous Rubble-Mound Breakwaters." MR 76-5. U. S. Army Corps of Engineers, Coastal Engineering Research Center, Fort Belvoir, Virginia. March 1976.

Pitt, J. D., and Ackers, P. "Prototype Tests on Riprap Under Random Wave Attack," Presented at the 18th Coastal Engineering Conference, Cape Town, South Africa. November 1982.

Thomsen, A. L., Wohlt, P. E., and Harrison, A. S. "Riprap Stability on Earth Embankments Tested in Large- and Small-Scale Wave Tanks." TM 37, U. S. Army Corps of Engineers, Coastal Engineering Research Center, Fort Belvoir, Virginia. June 1972.

U. S. Army Corps of Engineers. "Design of Coastal Revetments, Seawalls and Bulkheads." EM 1110-2-1614. 1984.

U. S. Army Corps of Engineers. "Earth Embankments." EM 1110-2-2300. 1971.

Vernard, J. K. and Street, R. L. Elementary Fluid Mechanics. 5th Edition. John Wiley and Sons, Inc. New York. 1976.

Vincent, C. L. "A Method for Estimating Depth-Limited Wave Energy." U. S. Army Corps of Engineers, Coastal Engineering Research Center, Coastal Engineering Technical Aid (CETA) 81-6, Fort Belvoir, Virginia.